WAVE LOADS AND MOTIONS OF LONG STRUCTURES IN DIRECTIONAL SEAS

by

OKEY U. NWOGU

B.A.Sc., University of Ottawa, 1983

A THESIS SUBMITTED IN PARTIAL FULFILMENT OF

THE REQUIREMENTS FOR THE DEGREE OF

MASTER OF APPLIED SCIENCE

in

FACULTY OF GRADUATE STUDIES

Department of Civil Engineering

We accept this thesis as conforming

to the required standard

THE UNIVERSITY OF BRITISH COLUMBIA

July 1985

In presenting this thesis in partial fulfilment of the requirements for an advanced degree at the THE UNIVERSITY OF BRITISH COLUMBIA, I agree that the Library shall make it freely available for reference and study. I further agree that permission for extensive copying of this thesis for scholarly purposes may be granted by the Head of my Department or by his or her representatives. It is understood that copying or publication of this thesis for financial gain shall not be allowed without my written permission.

Department of Civil Engineering

THE UNIVERSITY OF BRITISH COLUMBIA
2075 Wesbrook Place
Vancouver, Canada
V6T 1W5

Date: July 1985

ABSTRACT

The effects of wave directionality on the loads and motions of long structures is investigated in this thesis.

A numerical method based on Green's theorem is developed to compute the exciting forces and hydrodynamic coefficients due to the interaction of a regular oblique wave train with an infinitely long, semi-immersed floating cylinder of arbitrary shape. Comparisons are made with previous results obtained using other solution techniques. The results obtained from the solution of the oblique wave diffraction problem are used to determine the transfer functions and response amplitude operators for a structure of finite length and hence the loads and amplitudes of motion of the structure in short-crested seas.

The wave loads and body motions in short-crested seas are compared to corresponding results for long-crested seas. This is expressed as a directionally averaged, frequency dependent reduction factor for the wave loads and a response ratio for the body motions. Numerical results are presented for the force reduction factor and response ratio of a long floating box subject to a directional wave spectrum with a cosine power type energy spreading function. Applications of the results of the present procedure include such long structures as floating bridges and breakwaters.

Table of Contents

LIST OF TABLES

LIST OF FIGURES

NOMENCLATURE

a = half beam of cylinder

a_{ij} = matrix coefficient

A = displaced volume per unit length

A_o = complex amplitude of velocity potential

A_{ij} = complex wave amplitude

b = draft of cylinder

b_{ij} = matrix coefficient

B = beam of cylinder

c_{ij} = hydrostatic stiffness matrix coefficient

C_j = exciting force coefficient

$C(s), C'(s)$ = normalizing coefficients for directional spreading functions

d = water depth

f = circular frequency

$f_j^{(k)}$ = coefficient defined in eqn. (2.92)

F_j = exciting force

F_{ij} = force in the ith direction due to the jth mode of motion of cylinder

g = gravitational acceleration

$G(\omega,\beta)$ = directional spreading function

$G(\underline{x};\underline{\xi})$ = Green's function

H = incident wave height

H_j = system response function

i = $\sqrt{(-1)}$

I_o = polar mass moment of inertia about the y axis per unit length

k = incident wavenumber

K = Keulegan-Carpenter number

K_R, K_T = reflection and transmission coefficients

K_o, K_1 = modified Bessel functions of orders zero and one

l = length of structure

L = incident wavelength

m = mass per unit length of cylinder

m_{ij} = mass matrix coefficient

N = number of segments on $S_B+S_F+S_R$

$\underline{n}$ = unit normal vector directed out of fluid region

n_x, n_z = direction cosines of $\underline{n}$

p = pressure

$q(kl,\beta)$ = factor defined in eqn. (2.103)

r = distance between $\underline{x}$ and $\underline{\xi}$

r_y = radius of gyration of cylinder about the y axis

$r(kl,\beta)$ = reduction factor

r' = distance between $\underline{x}$ and $\underline{\xi}'$

R_F = force reduction factor

R_M = response ratio

s = cosine power of spreading function

$S(\omega)$ = spectral energy density

$S(\omega,\beta)$ = directional wave spectrum

S_B = immersed body surface

S_D = seabed

S_F = free surface

S_R = radiation surface

S_{11} = waterplane area moment of inertia about the x axis per unit length

t = time

T = wave period

$\underline{u}$ = fluid velocity vector

U = wind speed

U_m = maximum particle velocity

V = displaced volume of cylinder

V_n = normal velocity of body

x = horizontal coordinate normal to cylinder axis

$\underline{x}$ = vector of point (x,z)

x_f = centroid of the waterplane line measured from the centre of gravity

X_R = x coordinate of the radiation surface

y = horizontal coordinate parallel to cylinder axis

z = vertical coordinate measured upwards from the still water level

z_B = z coordinate of the centre of buoyancy

z_G = z coordinate of the centre of gravity

Z_j = response amplitude operator

β = angle of incidence measured from the positive x axis

β_o = principal direction of wave propagation

η = water surface elevation measured from the still water level

η_i = asymptotic wave amplitude

η_R, η_T = reflected and transmitted wave amplitudes

δ_{ij} = Kronecker delta function

Δ = phase angle

γ = angle between $\underline{x}-\underline{\xi}$ and $\underline{n}$; also Euler's constant

γ' = angle between $\underline{x}-\underline{\xi}'$ and $\underline{n}'$

λ_{ij} = damping coefficient

μ = nondimensional frequency parameter (see eqn. 2.14)

μ_{ij} = added mass coefficient

ν = nondimensional frequency parameter (see eqn. 2.14)

θ = angle of incidence measured from principal wave direction

ρ = density of fluid

Φ = velocity potential

ϕ_k = complex velocity potentials

ω = wave angular frequency

$\underline{\xi}$ = vector of point (ξ,ζ) on fluid boundary

$\underline{\xi}'$ = vector of point $[\xi,-(\zeta+2d)]$

ξ_j = nondimensional amplitude of body motion

Ξ_j = displacement or rotation of body

ζ_i = complex wave amplitude ratio

ACKNOWLEDGEMENTS

The author wishes to express his immense gratitude to Dr. Michael de St. Q. Isaacson for his guidance and advice throughout the preparation of this thesis.

Financial support in the form of a research assistantship from the Natural Sciences and Engineering Research Council of Canada is gratefully acknowledged.

1. INTRODUCTION

1.1 GENERAL

With the growth in the development of offshore resources, there has been a need for the safe and economic design of various offshore structures. An important aspect in the design of these structures involves the determination of both the exciting forces due to wave interaction with a fixed body and the response of the structure. The structure should be designed not only to withstand the the loads from the complex ocean environment, but in addition its motions generally have to be within acceptable limits.

The traditional approach to the design of offshore structures often assumes the incident wave field to be unidirectional or long-crested. Real seas are, however, both random and multi-directional, i.e. the waves not only have different amplitudes and frequencies but also may approach a structure from different directions. This property is also sometimes referred to as wave short-crestedness.

The directionality of the waves can significantly influence the loads and motions experienced by the structure. The use of directional spectra in wave force calculations often leads to a reduction in the computed forces, compared to the case of long-crested waves. This could lead to significant savings in construction costs. It could also affect decisions as to whether designs are accepted or rejected in feasibility studies. With the recent

developments in methods of determining directional wave spectra (Borgman (1969), Mitsuyasu *et al* (1975), Leblanc and Middleton(1982)) and the building of laboratory wave basins capable of generating directional waves, the use of directional spectra models is soon becoming an established part of the offshore design process.

When a wave train is incident upon an infinitely long semi-immersed structure, the structure responds in three degrees of freedom : heave (vertical motion), sway (beamwise motion), and roll (angular motion about the longitudinal axis). There are not only exciting forces due to the presence of the waves but also hydrodynamic forces associated with the response of the structure. For slender structures, the presence of the body does not significantly affect the incident wave kinematics and Morison's equation (Morison *et al*,1950) is often used to estimate the exciting forces. If the structure is large enough to diffract the incident wave field, flow separation effects are often neglected and the problem is solved using potential flow theory (Kellogg,1929). The complete problem is nonlinear and is usually linearized by assuming a small amplitude wave train.

A numerical method based on Green's theorem is used in this thesis to solve for the exciting forces and hydrodynamic coefficients of an infinite semi-immersed cylinder of arbitrary shape in oblique seas. The results are first extended to structures of finite length and then to

directional seas using the transfer function approach. The wave loads and motions of the structure in directional seas are compared with those of long-crested waves.

The applications of the results of this thesis include such long structures as floating breakwaters, floating bridges and pipelines. It could also be used in the study of ship motions where Korvin-Kroukovsky's (1955) strip theory is often used to reduce the three-dimensional problem to a two-dimensional one.

1.2 LITERATURE SURVEY

1.2.1 DIFFRACTION THEORY

A number of authors (Ursell (1949), MacCamy (1964), Kim (1965), Bai (1972), Ijima *et al* (1976)) have treated the two-dimensional wave-structure interaction problem. Much less work has however been reported for the case of obliquely incident waves.

Previous studies of oblique wave-structure interaction include those conducted by Black and Mei (1970), Bai (1975), Leonard *et al* (1983) for finite water depth, and by Garrison (1969), Bolton and Ursell (1973), and Garrison (1984) for infinite depth.

Garrison (1969) used a Green's function procedure to compute the exciting forces, added mass and damping coefficients, and reflection and transmission coefficients for a shallow draft cylinder floating at

the free surface. The method involves expressing the potential at any point in the fluid region in terms of a continuous distribution of sources along the body surface. The Green's function represents a point source of unit strength. The boundary condition on the body surface results in an integral equation which can be solved numerically to obtain the source strengths and hence the velocity potential. Garrison (1984) extended this approach to cylinders of arbitrary shape.

Bolton and Ursell (1973) used a multipole method to solve the problem associated with a circular cylinder oscillating in heave with the amplitude of motion varying sinusoidally along the length of the cylinder. The Haskind relations were then used to relate this radiation problem to the wave diffraction problem.

Black and Mei (1970) used a variational technique based on Schwinger's variational principle to obtain the far field solution of the problem. Bai (1975) also used a variational technique to solve for the exciting forces and reflection and transmission coefficients in water of finite depth. The method involves expressing the governing differential equation as the minimum of some functional. The fluid domain is divided into subregions and a set of interpolation functions with nodal variables is used to define the velocity potential over the domain. Minimising the functional with respect to the nodal variables yields a set of linear equations

which can be solved to give the potential field. The variational approach leads to a system of equations much larger than that of the integral equation method. The matrix is however symmetric and banded and can be solved using efficient techniques. Leonard *et al* (1983) used an approach similar to that of Bai (1975) in studying the case of multiple cylinders.

A boundary integral method involving Green's second identity is used in this thesis to solve the wave diffraction problem. The approach has previously been used by Ijima *et al* (1976) and Finnigan and Yammamoto (1979) for two-dimensional wave problems and by Isaacson (1981) for nonlinear wave-structure interaction. The present method avoids the complexity of deriving a Green's function which has to satisfy the various boundary conditions in water of finite depth. The results of the present procedure are compared with those of Bai (1975) for finite water depth, as well as Bolton and Ursell (1973) and Garrison (1984) for infinite water depth.

1.2.2 EFFECTS OF DIRECTIONAL WAVES

Previous studies of the loading and response of structures in directional seas are few and widely scattered in the literature.

There have been two general approaches used to determine the response of structures in short-crested

seas. The more common approach is the frequency domain approach where linear theories are used to determine transfer functions which relate the incident wave spectra to the response spectra.

Time domain simulations are often used when the wave-structure interaction process is of a nonlinear nature. Time domain description of directional seas involve either the digital filtering of white noise or Fast Fourier Transform (FFT) techniques. The time domain analysis is however generally more expensive than the frequency domain approach.

Huntington and Thompson (1976) computed the wave loads on a large vertical cylinder in short-crested seas. Linear diffraction theory was used to determine the transfer functions. The theoretical results were found to be in good agreement with experimental measurements.

Dean (1977) proposed a hybrid method of computing the wave loads on offshore structures which incorporates both the nonlinearity and directionality of the waves. A linearized form of Morison's equation was used to determine the effect of directional waves. Force reduction factors were presented for the cosine power spreading function.

Battjes (1982) studied the effects of directional waves on the loads on a long structure. Reduction factors were presented for a vertical wall occupying the

entire water depth and a pipeline for the cosine power type directional spreading function.

Dallinga *et al* (1984) investigated the effects of directional spreading on the loads and motions of a barge used for the transport of a jackup platform. Linear diffraction theory was used to obtain the transfer functions.

Bryden and Greated (1984) and Lambrakos (1982) both studied the response of long slender flexible horizontal cylinders in directional seas. Lambrakos (1982) used a finite number of wave frequencies and directions to describe the sea surface. The wave loads were determined from Morison's equation and the response of the structure was obtained by solving the differential equation of motion using a finite difference scheme.

Hackley (1979) and Shinozuka *et al* (1979) used a time domain approach to simulate the loading and response of structures in short-crested seas. The Fast Fourier Transform technique was used to determine the water particle velocities and accelerations for use in Morison's equation. Shinozuka *et al* (1979) found a reduction in the inline response in short-crested seas compared to long-crested seas. There was also a significant transverse response.

Georgiadis (1984) used a Monte Carlo simulation to determine the appropriate nodal forces on structures in short-crested seas. The response of the structure was

then evaluated using a deterministic analysis.

1.3 DESCRIPTION OF METHOD

The analysis of the dynamic response of long structures in directional seas can be divided into two parts.

The first part involves solving the problem of the diffraction of a regular oblique wave train by an infinite semi-immersed cylinder. An integral equation method based on Green's second identity is used to compute the exciting forces and hydrodynamic coefficients.

The fluid motion is described in terms of a velocity potential which consists of components due to the incident wave, diffracted wave, and forced waves for each mode of motion of the cylinder. Green's second identity is used to relate the values of the unknown velocity potentials and their normal derivatives on a boundary to the Green's function and its normal derivatives. The boundary consists of the immersed body surface, free surface and radiation surface. The Green's function only has to satisfy the governing differential equation which is the two-dimensional modified Helmholtz equation. The boundary is divided into a finite number of segments. Application of the various boundary conditions on the various surfaces yields a set of algebraic equations which can be solved to obtain the velocity potentials.

Bernoulli's equation is then used to compute the pressures and hence the exciting forces and hydrodynamic

forces due to the motions of the cylinder. The hydrodynamic forces can be expressed in terms of components in phase with the body acceleration and velocity. These are referred to as the added mass and damping coefficients respectively.

The reflection and transmission coefficients are determined by evaluating the asymptotic wave amplitudes at the radiation surface. Bernoulli's equation is used to relate the water surface elevation to the velocity potential with the pressure set to zero at the free surface.

The added mass and damping coefficients are then combined with the mass or moment of inertia of the body and the hydrostatic stiffness coefficients to obtain three coupled linear equations of motion for the body. The equations of motion are then solved to obtain the amplitudes of body motion per unit wave amplitude often referred to as the response amplitude operator.

For a rigid structure of finite length, the two-dimensional forces are integrated along the body axis to obtain the total wave loads on the structure.

The second part of the analysis involves extending the results for a regular oblique wave train to random multi-directional seas using the linear transfer function approach. The short-crested sea surface is described in terms of a directional wave spectrum. The directional wave spectrum can be expressed as the product of the conventional one-dimensional frequency spectrum and a directional spreading function. A cosine power spreading function which

is independent of frequency is used in this study.

The exciting force and body response spectra are obtained by multiplying the incident wave spectrum with the appropriate transfer function or response amplitude operator. The effects of wave directionality is expressed as a directionally averaged, frequency dependent reduction factor to be applied to the one-dimensional force spectrum. The mean square values of the response in short-crested seas are also compared to corresponding results for long-crested seas.

2. DIFFRACTION THEORY

2.1 INTRODUCTION

Before treating the problem of the dynamic response of long structures in multi-directional seas, we shall first consider the interaction of a regular oblique wave train with an infinite semi-immersed horizontal cylinder of arbitrary shape.

The cylinder is considered large enough so as to diffract the incident flow field. Flow separation effects are assumed negligible and the effects of viscosity are assumed confined to a thin boundary layer on the body surface. The fluid flow can thus be considered to be irrotational and the problem solved using potential flow theory. An indication of the importance of flow separation effects is the Keulegan-Carpenter number, K. The Keulegan-Carpenter number is defined as the ratio of the amplitude of fluid motion to a typical dimension of the body, that is

$$K = U_m T/B \tag{2.1}$$

where U_m is the maximum particle velocity, T is the wave period and B is a typical dimension of the body. For the range of frequencies used in this study, K will usually be less than two and flow separation should not occur (see Sarpkaya and Isaacson,1981).

For rectangular section cylinders which are used in this study, vortices are usually formed at the sharp

corners. Various authors (Bearman *et al* (1979), Mogridge and Jamieson (1976)) have however found good agreement between potential flow theory and experimental results for such cylinders when fixed despite the formation of the vortices. For floating cylinders, the roll amplitude of motion is significantly affected by viscous damping particularly near the resonance frequency and an empirical viscous damping coefficient should be included in the equations of motion.

It is usually convenient to separate the wave-structure interaction problem for floating bodies into two parts: (1) exciting forces due to wave diffraction by a fixed cylinder, and (2) hydrodynamic forces associated with an infinite cylinder oscillating in heave, sway and roll in an otherwise still water expressed in terms of added mass and damping coefficients. The wave height and oscillatory motions of the cylinder are assumed small so that the complete problem of wave interaction with a floating cylinder can be represented by a linear superposition of the diffraction and forced motion problems.

The cylinder is assumed flexible with its amplitude of oscillation periodic along the axis of the cylinder, so the three-dimensional problem can be reduced to a two-dimensional one. Even though the numerical results are obtained for an infinite cylinder, they are extended to structures of finite length by integrating along the body axis, ignoring end effects. For non-uniform bodies such as ships, Korvin-Kroukovsky's (1955) strip theory can be used

with the two-dimensional results. For head seas (wave crests normal to the cylinder axis), the wavelength along the length of the cylinder becomes of the same order of magnitude as a typical cross sectional dimension and the procedure is no longer applicable. A three-dimensional model which considers end effects would have to be used as the incident wave direction moves substantially away from the beam direction.

2.2 THEORETICAL FORMULATION

2.2.1 WAVE DIFFRACTION PROBLEM

A regular small amplitude wave train of height H and angular frequency ω is obliquely incident upon an infinitely long fixed horizontal cylinder. The waves propagate in water of depth d in a direction making an angle β with the x axis (see Fig. 1). The coordinate system is right handed with z measured upwards from the still water level and the x-y plane horizontal. The y axis is parallel to the axis of the infinite cylinder. The origin of the (x,y,z) coordinate system is at the still water level vertically above or below the centre of gravity. The fluid is assumed to be inviscid and incompressible and the flow irrotational. The fluid motion may therefore be described in terms of a velocity potential Φ, defined by

$$\underline{u} = \nabla\Phi(x,y,z,t) \qquad (2.2)$$

where $\underline{u}$ is the fluid velocity vector and Φ must satisfy the Laplace equation

$$\nabla^2\Phi(x,y,z,t) = 0 \tag{2.3}$$

within the fluid region. The wave height is assumed sufficiently small so that linear wave theory is applicable and consequently Φ is subject to the usual linearized boundary conditions.

On the free surface, the dynamic pressure is given by the Bernoulli equation

$$\frac{\partial\Phi}{\partial t} + g\eta + \frac{1}{2}(\nabla\Phi)^2 = R \tag{2.4}$$

where g is the gravitational acceleration and R is the Bernoulli constant set equal to zero for convenience.

The kinematic free surface boundary condition requires that the normal velocity of the free surface elevation be equal to the normal velocity of a fluid particle at the free surface. This can be expressed as

$$\frac{\partial\Phi}{\partial z} = \frac{\partial\eta}{\partial t} + \frac{\partial\Phi}{\partial x}\frac{\partial\eta}{\partial x} + \frac{\partial\Phi}{\partial y}\frac{\partial\eta}{\partial y} \tag{2.5}$$

Eqns. (2.4) and (2.5) are linearized by neglecting the fluid velocity square term in eqn. (2.4) and the wave steepness terms in eqn. (2.5), and by applying the conditions at the still water level z=0 rather than at the instantaneous water surface elevation $z=\eta$. The two equations can then be combined to give the linearized free surface boundary condition

$$\frac{\partial \Phi}{\partial z} - \frac{\omega^2}{g}\Phi = 0 \qquad \text{at } z=0 \qquad (2.6)$$

for simple harmonic motion.

The immersed body surface is assumed impermeable and hence the normal velocity of the fluid on the body surface, S_B must equal zero

$$\frac{\partial \Phi}{\partial n} = 0 \qquad \text{on } S_B \qquad (2.7)$$

where n is a direction normal to the body surface directed into the body. The seabed is assumed horizontal and impermeable giving

$$\frac{\partial \Phi}{\partial z} = 0 \qquad \text{at } z=-d \qquad (2.8)$$

In addition to the above boundary condtions, Φ has to satisfy a radiation condition at the far field to ensure a unique solution.

It is convenient to assume the velocity potential to be of the form

$$\Phi = \Phi_0 + \Phi_4 \qquad (2.9)$$

where Φ_0 and Φ_4 are the velocity potentials for the incident and diffracted waves respectively. The incident wave potential is given by linear wave theory as

$$\Phi_0(x,y,z,t) = \mathrm{Re}\left[\frac{-igH}{2\omega}\,\frac{\cosh[k(z+d)]}{\cosh(kd)} \times \exp\{i(kx\cos\beta+ky\sin\beta-\omega t)\}\right] \qquad (2.10)$$

where k is the wave number which is related to the angular frequency ω by the dispersion relation

$$k \tanh(kd) = \frac{\omega^2}{g} \tag{2.11}$$

The radiation condition which ensures that the diffracted waves are travelling away from the cylinder is given by

$$\frac{\partial \Phi_4}{\partial x} \mp ik\cos\beta\ \Phi_4 = 0 \qquad \text{at } x = \pm\infty \tag{2.12}$$

In a numerical approximation, the infinite boundary is truncated at a finite distance, X_R from the origin where the evanescent modes due to the presence of the the body are assumed to have decayed sufficiently. An approximate analysis to find the optimum distance X_R at which the radiation condition is applied is given in appendix I.

The fluid motion is considered periodic in time as well as along the axis of the cylinder. A nondimensional potential, ϕ can thus be defined by

$$\Phi(x,y,z,t) = \mathrm{Re}\left[\frac{-igH}{2\omega}\phi(x,z)\exp\{i(ky\sin\beta - \omega t)\}\right] \tag{2.13}$$

It is also convenient to nondimensionalize the variables using the half beam of the cylinder, a.

$$\left.\begin{aligned} x' &= x/a, \quad z' = z/a, \quad y' = y/a, \quad k' = ka \\ d' &= d/a, \quad \mu = \frac{\omega^2 a}{g}, \quad \nu = ka\sin\beta \end{aligned}\right\} \tag{2.14}$$

For convenience, the primes have been dropped from the variables and it is understood that the variables are now nondimensional. Dimensional variables will henceforth be barred where necessary for clarity.

The boundary value problem for the diffracted potential can now be stated in nondimensional form as

$$\nabla^2\phi_4 - \nu^2\phi_4 = 0 \qquad \text{in the fluid} \qquad (2.15a)$$

$$\frac{\partial\phi_4}{\partial n} = \mu\phi_4 \qquad \text{at } z=0 \qquad (2.15b)$$

$$\frac{\partial\phi_4}{\partial n} = 0 \qquad \text{at } z=-d \qquad (2.15c)$$

$$\frac{\partial\phi_4}{\partial n} = ik\cos\beta\phi_4 \qquad \text{at } x=\pm X_R \qquad (2.15d)$$

$$\frac{\partial\phi_4}{\partial n} = -\frac{\partial\phi_0}{\partial n} \qquad \text{on } S_B \qquad (2.15e)$$

where

$$\phi_0 = \frac{\cosh[k(z+d)]}{\cosh(kd)} \exp(ikx\cos\beta) \qquad (2.16)$$

The three-dimensional Laplace equation (2.3) has now been reduced to the two-dimensional modified Helmholtz equation (2.15a).

2.2.2 FORCED MOTION PROBLEM

Consider an infinitely long cylinder oscillating in heave, sway and roll as shown in Fig. 2. Each mode of motion is periodic in time as well as along the axis of the cylinder. The displacement or rotation in the kth mode is given by

$$\Xi_k(y,t) = \begin{Bmatrix} a \\ 1 \end{Bmatrix} \mathrm{Re}[\xi_k \exp\{i(\nu y - \omega t)\}] \qquad \begin{Bmatrix} k = 1,2 \\ k = 3 \end{Bmatrix} \qquad (2.17)$$

where ξ_k is the complex amplitude of oscillation of the cylinder with k=1,2,3 corresponding to the sway, heave and roll modes respectively. Throughout the following

development, the upper terms in the curly brackets apply with each other, and separately the lower terms apply with each other. ξ_1 and ξ_2 have been nondimensionalized by a, while ξ_3 corresponds to the roll angle in radians.

The velocity of the body surface in the direction $\underline{n}$ is given by

$$V_n = \sum_{k=1}^{3} \frac{\partial \Xi}{\partial t} n_k = \mathrm{Re}\left[\sum_{k=1}^{3} -i\omega a \xi_k n_k \exp\{i(\nu y - \omega t)\} \right] \qquad (2.18)$$

where

$$\left.\begin{aligned} n_1 &= n_x \\ n_2 &= n_z \\ n_3 &= (z-e)n_x - x n_z \end{aligned}\right\} \qquad (2.19)$$

and n_x, n_z are the direction cosines of the unit normal vector $\underline{n}$ on the immersed body surface and (0,e) denotes the point about which the roll motion is prescribed. The normal velocity of the fluid on the immersed body surface must equal the normal velocity of the body yielding

$$\frac{\partial \Phi}{\partial \bar{n}} = V_n \qquad \text{on } S_B \qquad (2.20)$$

This boundary condition is satisfied at the equilibrium position of the body rather than at the instantaneous position of the body.

From equations (2.18) and (2.20), the forced motion potential for the kth mode of motion can be expressed as

$$\Phi_k = \mathrm{Re}[-i\omega a^2 \xi_k \phi_k \exp\{i(\nu y - \omega t)\}] \qquad (2.21)$$

The linearized boundary condition on the body surface can thus be expressed as

$$\frac{\partial \phi_k}{\partial n} = n_k \qquad k=1,2,3 \qquad (2.22)$$

The boundary value problem for the forced motion potentials $\phi_k (k=1,2,3)$ is hence governed by eqns. (2.15a-d) and eqn. (2.22).

2.3 GREEN'S FUNCTION SOLUTION

A boundary integral method involving Green's identity is used as the basis for the numerical evaluation of the potentials $\phi_k (k=1,2,3,4)$. The second form of Green's theorem may be applied over a closed surface S containing the fluid region in order to relate the values of the potential $\phi(\underline{x})$ in the fluid region to the boundary values of the potential $\phi(\underline{\xi})$ and its normal derivative $\partial\phi(\underline{\xi})/\partial n$. This can be expressed as

$$\phi(\underline{x}) = \frac{1}{2\pi} \int_S [\phi(\underline{\xi}) \frac{\partial G}{\partial n}(\underline{x};\underline{\xi}) - \frac{\partial \phi}{\partial n}(\underline{\xi}) G(\underline{x};\underline{\xi})] dS \qquad (2.23)$$

where $G(\underline{x};\underline{\xi})$ is an appropriate Green's function, $\underline{x}$ denotes the point (x,z) being considered and $\underline{\xi}$ denotes the point (ξ,ζ) over which the integration is performed. The closed surface S comprises the immersed body surface S_B, the mean free surface S_F, the radiation surface S_R, and the seabed S_D as shown in Fig. 3.

When the interior point $\underline{x}$ approaches the boundary from within, eqn. (2.23) reduces to the following integral

equation

$$\phi(\underline{x}) = \frac{1}{\pi}\int_S [\phi(\underline{\xi})\frac{\partial G}{\partial n}(\underline{x};\underline{\xi}) - \frac{\partial \phi}{\partial n}(\underline{\xi})G(\underline{x};\underline{\xi})]dS \qquad (2.24)$$

The Green's function which satisfies the modified Helmholtz equation (2.15a) in an unbounded fluid and is singular at the point $\underline{x}=\underline{\xi}$ is given by

$$G(\underline{x};\underline{\xi}) = -K_0(\nu r) \qquad (2.25)$$

where K_0 is the modified Bessel function of order zero and r is the distance between the points $\underline{x}$ and $\underline{\xi}$

$$r = |\underline{\xi} - \underline{x}| = [(\xi-x)^2 + (\zeta-z)^2]^{1/2} \qquad (2.26)$$

The function $K_0(x) \simeq -\ln x$ as $x \to 0$. The Green's function which satisfies the two-dimensional Laplace equation

$$G(\underline{x};\underline{\xi}) = \ln r \qquad (2.27)$$

is thus obtained as $\beta \to 0°$.

Since the seabed is assumed horizontal, it is computationally more efficient to exclude the seabed from S and an alternative Green's function which takes into account symmetry about the seabed can be defined

$$G(\underline{x};\underline{\xi}) = -[K_0(\nu r) + K_0(\nu r')] \qquad (2.28)$$

where r' is the distance between the points $\underline{x}$ and $\underline{\xi}' = (\xi,-(\zeta+2d))$ which is the reflection of $\underline{\xi}$ about the seabed:

$$r' = |\underline{\xi}' - \underline{x}| = [(\xi-x)^2 + (\zeta+2d+z)^2]^{1/2} \qquad (2.29)$$

If the depth variations are significant, the seabed would have to be included in S and the Green's function given by eqn. (2.25) used instead.

The integral equation (2.24) can now be evaluated numerically to give the potential ϕ at any point in the fluid and hence provide the solution to the boundary value problem.

2.4 EXCITING FORCES, ADDED MASSES AND DAMPING COEFFICIENTS

Once the velocity potential is obtained, the hydrodynamic pressure can be computed from the linearized Bernoulli equation

$$p = -\rho\frac{\partial\Phi}{\partial t} = i\omega\rho\Phi \tag{2.30}$$

The forces and moments per unit length are determined by integrating the hydrodynamic pressure over the immersed body surface S_B.

The exciting force per unit length which is due to the incident and scattered waves and is proportional to the wave height is given by

$$F_j = i\omega\rho\begin{Bmatrix}a\\a_2\end{Bmatrix}\int_{S_B}\Phi n_j dS \qquad \begin{Bmatrix}j = 1,2\\ j = 3\end{Bmatrix} \tag{2.31}$$

where $F_j(j=1,2)$ denotes the sway and heave force respectively while F_3 denotes the roll moment. Substitution of equations (2.9) and (2.13) into eqn. (2.31) yields

$$F_j(y,t) = \rho g\frac{H}{2}\begin{Bmatrix}a\\a_2\end{Bmatrix}\mathrm{Re}\left[\int_{S_B}(\phi_0+\phi_4)n_j\exp\{i(\nu y-\omega t)\}dS\right]\begin{Bmatrix}j=1,2\\ j=3\end{Bmatrix} \tag{2.32}$$

The dimensionless exciting force amplitude is given by

$$C_j = \frac{F_j(y,t)}{\frac{1}{2}\rho g H a^2}\begin{Bmatrix} a \\ 1 \end{Bmatrix} = \int_{S_B} (\phi_0+\phi_4) n_j \, dS \qquad \begin{Bmatrix} j=1,2 \\ j=3 \end{Bmatrix} \tag{2.33}$$

The exciting force could alternatively be defined by

$$\frac{F_j(y,t)}{\frac{1}{2}\rho g H a^2}\begin{Bmatrix} a \\ 1 \end{Bmatrix} = |C_j| \cos(\nu y - \omega t + \Delta_j) \qquad \begin{Bmatrix} j=1,2 \\ j=3 \end{Bmatrix} \tag{2.34}$$

where the phase angle Δ_j is defined by

$$\Delta_j = \tan^{-1}\left[\frac{Im(C_j)}{Re(C_j)}\right] \tag{2.35}$$

There are also hydrodynamic forces associated with the motions of the cylinder which are proportional to the amplitude of cylinder motion. The ith component of the force due to the jth component of motion can be expressed as

$$F_{ij} = i\omega\rho\begin{Bmatrix} a \\ a^2 \end{Bmatrix} \int_{S_B} \Phi_j n_i \, dS \qquad \begin{Bmatrix} i=1,2 \\ i=3 \end{Bmatrix} \quad j=1,2,3 \tag{2.36}$$

Substitution of the equation for the forced motion potentials (2.21) into eqn. (2.36) yields

$$F_{ij} = \rho\omega^2 \xi_j \begin{Bmatrix} a^3 \\ a^4 \end{Bmatrix} Re\left[\int_{S_B} \phi_j n_i \exp\{i(\nu y - \omega t)\} dS\right] \qquad \begin{Bmatrix} i=1,2 \\ i=3 \end{Bmatrix} \quad j=1,2,3 \tag{2.37}$$

This force can also be expressed in terms of two components; one component in phase with the acceleration and the other in phase with the velocity

$$F_{ij} = -\mu_{ij}\ddot{\Xi}_j - \lambda_{ij}\dot{\Xi}_j \qquad j=1,2,3 \tag{2.38}$$

where μ_{ij} and λ_{ij} are the added mass and damping

coefficients respectively. Substitution of eqn. (2.17) into eqn. (2.38) gives

$$F_{ij} = \begin{Bmatrix} a \\ 1 \end{Bmatrix} \mathrm{Re}[(\omega^2 \mu_{ij} \xi_j + i\omega\lambda_{ij}\xi_j)\exp\{i(\nu y - \omega t)\}] \qquad \begin{Bmatrix} j=1,2 \\ j=3 \end{Bmatrix} \quad i=1,2,3 \tag{2.39}$$

Comparing eqn. (2.37) with eqn (2.39) gives the nondimensional added mass and damping coefficients as

$$\frac{\mu_{ij}}{\rho a^m} = \mathrm{Re}\left[\int_{S_B} \phi_j n_i \, dS\right] \tag{2.40}$$

$$\frac{\lambda_{ij}}{\rho\omega a^m} = \mathrm{Im}\left[\int_{S_B} \phi_j n_i \, dS\right] \tag{2.41}$$

where the constant m is given as

$$m = \begin{cases} 2 \text{ for } (i,j) = (1,1) \text{ and } (2,2) \\ 3 \text{ for } (i,j) = (1,3) \text{ and } (3,1) \\ 4 \text{ for } (i,j) = (3,3) \end{cases} \tag{2.42}$$

The Haskind (1953) relations (also see Newman,1962) provide an alternate way of calculating the exciting forces. Applying Green's theorem to the diffraction potential gives

$$\int_{S_B} \left(\phi_j \frac{\partial \phi_4}{\partial n} - \phi_4 \frac{\partial \phi_j}{\partial n}\right) dS = 0 \qquad j=1,2,3 \tag{2.43}$$

Substituting the above expression into eqn. (2.32) gives

$$C_j = \int_{S_B} \left(\phi_0 \frac{\partial \phi_j}{\partial n} + \phi_j \frac{\partial \phi_4}{\partial n}\right) dS \tag{2.44}$$

Applying the boundary condition given by eqn. (2.15e) eliminates the diffraction potential from the expression for the exciting force

$$C_j = \int_{S_B} (\phi_o \frac{\partial \phi_j}{\partial n} - \phi_j \frac{\partial \phi_o}{\partial n}) dS \qquad (2.45)$$

There is also a direct relation between the damping coefficient and the amplitude of the waves generated by an oscillating cylinder symmetrical about x=0. An amplitude ratio $|\zeta_i|$ can be defined as the ratio of the wave amplitude at $|x|=\infty$ to the amplitude of oscillation of the cylinder, that is

$$|\zeta_i| = \frac{|\eta_i|}{|a\xi_i|} \qquad (2.46)$$

where $|\eta_i|$ is the amplitude of the radiated waves at $|x|=\infty$ for the ith mode of oscillation of the cylinder.

By equating the work done in oscillating the cylinder to the energy flux radiated across a control surface at infinity, it can be shown that (see Newman,1977)

$$\frac{\lambda_{ij}}{\rho\omega a^m} = [1 + \frac{2kd}{\sinh 2kd}] \frac{\cos\beta}{(ka)^2 \tanh kd} |\zeta_i|^2 \qquad (2.47)$$

for the oblique case. The exciting force can also be related to the amplitude ratio by evaluating the integral in eqn. (2.45) at the negative radiation surface ($x=-X_R$). The integral does not vanish since the incident wave potential does not satisfy the radiation condition. Since the forced motion potential is proportional to the square root of the energy flux, eqn. (2.45) can be integrated over the depth at $x=-X_R$ to give the exciting force coefficient as

$$|C_i| = = [1 + \frac{2kd}{\sinh 2kd}] \frac{\cos\beta}{ka} |\zeta_i| \qquad (2.48)$$

Equations (2.47) and (2.48) can be combined to provide a direct relation between the exciting force coefficients and the damping coefficients

$$|C_i| = \left[\frac{\lambda_{ij}}{\rho\omega a^m} \left(1 + \frac{2kd}{\sinh 2kd}\right) \tanh kd \cos\beta \right]^{1/2} \qquad (2.49)$$

Equations (2.47)-(2.49) provide a useful check on the numerical results obtained.

2.5 EQUATIONS OF MOTION

The dynamic response of the cylinder due to the exciting waves can now be obtained by solving the equations of motion. The equations of motion are of the form

$$\sum_{j=1}^{3} [-\omega^2(m_{ij}+\mu_{ij}) - i\omega\lambda_{ij} + c_{ij}]\Xi_j = F_i(y,t) \quad i=1,2,3 \qquad (2.50)$$

where m_{ij} and c_{ij} are the mass and hydrostatic stiffness matrix coefficients respectively. Additional forces due to moorings or viscous damping may be included in eqn. (2.50) if present. It should be noted that for the case of roll motion, nonlinear viscous damping is important particularly near the resonance frequency and would have to be included in practical applications.

It was assumed in deriving the added mass and damping coefficients that the cylinder was flexible with its amplitude of motion varying sinusoidally along the length of the cylinder as well as in time. The term $\sin\beta$ can be thought of as the ratio of the incident wave length to the

the wave length along the axis of the cylinder. A rigid cylinder has an infinite wavelength along the axis of the cylinder and hence corresponds to a flexible cylinder with $\beta=0°$.

The components of the mass matrix are given as

$$m_{ij} = \begin{bmatrix} m & 0 & -mz_G \\ 0 & m & 0 \\ -mz_G & 0 & I_o \end{bmatrix} \tag{2.51}$$

where m is the mass per unit length of the body, z_G is the z coordinate of the centre of gravity and I_o is the polar mass moment of inertia about the y axis per unit length. I_o may be expressed as

$$I_o = m(r_y^2 + z_G^2) \tag{2.52}$$

where r_y is the radius of gyration of the body about the y axis. The hydrostatic stiffness matrix is determined by calculating the forces required to restore the body to its equilibrium position for small amplitude displacements. The stiffness matrix components are given as

$$c_{ij} = \begin{bmatrix} 0 & 0 & 0 \\ 0 & c_{22} & c_{23} \\ 0 & c_{23} & c_{33} \end{bmatrix} \tag{2.53}$$

where

$$c_{22} = \rho g B \tag{2.54a}$$

$$c_{23} = \rho g B x_f \tag{2.54b}$$

$$c_{33} = \rho g A[(S_{11}/A) + z_B - z_G] \qquad (2.54c)$$

where B is the beam of the cylinder, x_f is the centroid of the waterplane line and is equal to zero for bodies symmetrical about x=0, z_B is the z coordinate of the centre of buoyancy, A is the displaced volume per unit length, and S_{11} is the waterplane area moment of inertia about the x axis per unit length, that is

$$S_{11} = \int_B x^2 dx = B^3/12 \qquad (2.55)$$

Static stability in roll requires that the coefficient c_{33} be positive. From eqn. (2.54c), it is evident that the metacentre $(S_{11}/A) + z_B$ has to be located higher than the centre of gravity z_G for the floating body to be stable.

The equations of motion (2.50) can now be solved to obtain the complex amplitudes of oscillation, ξ_j for any given wave frequency and direction using a complex matrix inversion technique. The amplitude of body motion is often described in terms of the response amplitude operator defined as

$$Z_j(\omega,\beta) = \frac{|a\xi_j|}{H/2} \qquad (2.56)$$

The response amplitude operator represents the amplitude of body motion due to a unit amplitude wave of frequency ω, travelling in direction β.

2.6 REFLECTION AND TRANSMISSION COEFFICIENTS

Another two quantities of physical interest especially for such structures as floating breakwaters are the reflection and transmission coefficients. The coefficients are obtained by evaluating the component wave amplitudes at the radiation surfaces ($x=\pm X_R$). There are contributions to this asymptotic wave amplitude from: (1) the oscillations of the cylinder in its three modes, and (2) the reflection and transmission of the incident wave by a fixed body.

From Bernoulli's equation, the wave amplitude is related to the velocity potential by

$$\eta = -\frac{1}{g}\frac{\partial \Phi}{\partial t}(x,y,0,t) \tag{2.57}$$

Substituting the equation for the forced motion potentials (2.21) into eqn. (2.57) yields the asymptotic wave amplitude for each mode of motion

$$\eta_i = \mathrm{Re}\left[\frac{\omega^2}{g}a^2\xi_i\phi_i(x,0)\exp\{i(\nu y-\omega t)\}\right] \tag{2.58}$$

The wave amplitude ratio previously defined by eqn. (2.46) is now given as

$$|\zeta_i| = \frac{|\eta_i|}{|a\xi_i|} = \frac{\omega^2 a}{g}|\phi_i(x,0)| \tag{2.59}$$

evaluated at $x=\pm X_R$. At the radiation surface, the evanescent modes are assumed to have decayed sufficiently (see appendix I) and the velocity potentials are of the form

$$\phi(x,z) = A_o\frac{\cosh[k(z+d)]}{\cosh(kd)}\exp(\pm ikx\cos\beta) \quad \text{at } x = \pm X_R \tag{2.60}$$

where A_0 is the complex amplitude of the potential at z=0. Given that

$$\int_{-d}^{0} \cosh^2[k(z+d)]dz = \frac{\sinh(2kd) + 2kd}{4k} \tag{2.61}$$

the coefficient A_0 can be obtained by applying the orthogonality condition of the hyperbolic cosine function and is given for the jth potential as

$$A_{0j} = \frac{4k\cosh(kd)}{\sinh(2kd) + 2kd} \exp(\pm ikx\cos\beta) \int_{-d}^{0} \phi_j \cosh[k(z+d)]dz \quad \text{at } x=\mp X_R \tag{2.62}$$

The wave amplitude ratio can thus be evaluated as

$$|\zeta_j| = \frac{\omega^2 a}{g}|A_{0j}| \tag{2.63}$$

for each mode of motion. The reflection and transmission coefficients due to the presence of a fixed body are obtained in a similar manner. The reflection coefficient can be obtained by evaluating the asymptotic wave amplitude of the scattered waves at the negative radiation surface ($x=-X_R$). Substitution of the form of the diffracted wave potential given by eqn. (2.13) into eqn. (2.57) yields

$$\eta_R = \mathrm{Re}[\tfrac{H}{2}\phi_4(-X_R,0)\exp\{i(\nu y-\omega t)\}] \tag{2.64}$$

The reflection coefficient is defined as the ratio of the reflected wave amplitude to the incident wave amplitude and is thus given by

$$K_R = \frac{|\eta_R|}{H/2} = |\phi_4(-X_R,0)| \tag{2.65}$$

The transmission coefficient is due to the asymptotic wave amplitude of the incident and scattered waves at the positive radiation surface ($x=X_R$) and is similarly given by

$$K_T = |\phi_0(X_R,0) + \phi_4(X_R,0)| \tag{2.66}$$

The expressions on the right side of eqns. (2.65) and (2.66) are evaluated using eqn. (2.62).

Applying conservation of energy principles, remembering that the energy in a wave is proportional to the square of the wave amplitude, the reflection and transmission coefficients are related by

$$K_R^2 + K_T^2 = 1 \tag{2.67}$$

After obtaining the amplitudes of body motion by solving the equations of motion, the reflection and transmission coefficients for a freely floating body are determined respectively as

$$K_R = |\phi_4(-X_R,0) + \sum_{j=1}^{3} \zeta_j Z_j(\omega,\beta)| \tag{2.68a}$$

$$K_T = |\phi_0(X_R,0) + \phi_4(X_R,0) + \sum_{j=1}^{3} \zeta_j Z_j(\omega,\beta)| \tag{2.68b}$$

2.7 NUMERICAL PROCEDURE

In order to evaluate the integral equation (2.24), the boundary is divided into N segments with the value of ϕ or $\partial\phi/\partial n$ considered constant over each segment and equal to the value at the midpoint of the segment. Eqn. (2.24) can be replaced by the summation equation

$$\phi_k(\underline{x}_i) = \frac{1}{\pi}\sum_{j=1}^{N}\{\phi_k(\underline{x}_j)\int_{\Delta S_j}\frac{\partial G}{\partial n}(\underline{x}_i;\underline{x}_j)dS - \frac{\partial \phi_k}{\partial n}\int_{\Delta S_j} G(\underline{x}_i;\underline{x}_j)dS\} \qquad k=1,2,3,4 \qquad (2.69)$$

where the summation in eqn. (2.69) is performed in a counter clockwise manner around the boundary. Eqn. (2.69) can be rewritten as

$$\sum_{j=1}^{N}\{(a_{ij}+\delta_{ij})\phi_j^{(k)} + b_{ij}\frac{\partial \phi_j^{(k)}}{\partial n}\} = 0 \qquad k=1,2,3,4 \qquad (2.70)$$

where δ_{ij} is the Kronecker delta function given by

$$\delta_{ij} = \begin{cases} 1 & i=j \\ 0 & i\neq j \end{cases} \qquad (2.71)$$

The coefficients a_{ij} and b_{ij} are defined as

$$a_{ij} = \frac{1}{\pi}\int_{\Delta S_j}\frac{\partial}{\partial n}[K_o(\nu r_{ij}) + K_o(\nu r'_{ij})]dS \qquad (2.72)$$

$$b_{ij} = -\frac{1}{\pi}\int_{\Delta S_j}[K_o(\nu r_{ij}) + K_o(\nu r'_{ij})]dS \qquad (2.73)$$

r_{ij} and r'_{ij} are given as

$$r_{ij} = [(x_j-x_i)^2 + (z_j-z_i)^2]^{1/2} \qquad (2.74)$$

$$r'_{ij} = [(x_j-x_i)^2 + (z_j+2d+z_i)^2]^{1/2} \qquad (2.75)$$

$\underline{x}_i$ and $\underline{x}_j$ are evaluated at the midpoint of each segment. The gradient $\partial G/\partial n$ may be expressed as

$$\frac{\partial G}{\partial n}(\underline{x}_i;\underline{x}_j) = \frac{\partial G}{\partial r}\cos\gamma + \frac{\partial G}{\partial r'}\cos\gamma' \qquad (2.76)$$

where γ and γ' are as shown in Fig. 4 and correspond to the angles between $\underline{n}_j$ and $\underline{r}=\underline{x}_j-\underline{x}_i$, and between $\underline{n}'_j$ and $\underline{r}'=\underline{x}'_j-\underline{x}_i$ respectively, that is

$$\cos\gamma = \frac{\underline{n}_j \cdot (\underline{x}_j - \underline{x}_i)}{r} \tag{2.77}$$

$$\cos\gamma' = \frac{\underline{n}'_j \cdot (\underline{x}'_j - \underline{x}_i)}{r} \tag{2.78}$$

$$\text{where } \underline{n}_j = n_x \underline{i} + n_z \underline{k}$$
$$\underline{n}'_j = n_x \underline{i} - n_z \underline{k} \tag{2.79}$$

and $\underline{x}'_j$ is the point $(x_j, -(z_j+2d))$. The unit normal vector $\underline{n}$ is given by

$$\underline{n} = \frac{\partial z}{\partial S}\,\underline{i} - \frac{\partial x}{\partial S}\,\underline{k} \tag{2.80a}$$

The above expression can be approximated as

$$\underline{n} = \frac{\Delta z}{\Delta S}\,\underline{i} - \frac{\Delta x}{\Delta S}\,\underline{k} \tag{2.80b}$$

The derivative of the Green's function is given by

$$\frac{\partial}{\partial r} K_0(\nu r) = -\nu K_1(\nu r) \tag{2.81}$$

where K_1 is the modified Bessel function of order one. When $i \neq j$, the integrals in eqns. (2.72) and (2.73) are approximated by evaluating the Green's function and its normal derivative at the midpoint of each segment. The coefficient a_{ij} is thus given as

$$a_{ij} = -\nu \frac{K_1(\nu r_{ij})}{\pi r_{ij}} [(x_j - x_i) n_x + (z_j - z_i) n_z] \Delta S_j$$
$$- \nu \frac{K_1(\nu r'_{ij})}{\pi r'_{ij}} [(x_j - x_i) n_x + (z_j + 2d + z_i) n_z] \Delta S_j \quad i \neq j \tag{2.82a}$$

Substituting the approximation for the direction cosines given in eqn. (2.80b), a_{ij} becomes

$$a_{ij} = -\nu\frac{K_1(\nu r_{ij})}{\pi r_{ij}}[(x_j-x_i)\Delta z_j - (z_j-z_i)\Delta x_j]$$
$$- \nu\frac{K_1(\nu r'_{ij})}{\pi r'_{ij}}[(x_j-x_i)\Delta z_j - (z_j+2d+z_i)\Delta x_j] \quad i\neq j \quad (2.82b)$$

where $\Delta z_j = z_{j+1} - z_j$

$\Delta x_j = x_{j+1} - x_j$

$\Delta S_j = [(\Delta z_j)^2 + (\Delta x_j)^2]^{1/2}$

The coefficient b_{ij} is given as

$$b_{ij} = -\frac{1}{\pi}[K_0(\nu r_{ij}) + K_0(\nu r'_{ij})]\Delta S_j \qquad i\neq j \qquad (2.83)$$

When i=j, the integrals in eqns. (2.72) and (2.73) become singular. Evaluating the nonsingular components $K_0(\nu r')$ and $\partial K_0(\nu r')/\partial n$ as before and using the asymptotic formula for $K_0(\nu r)$ (see Abramowitz and Stegun,1964)

$$K_0(\nu r) \simeq -\{\ln(\nu r/2) + \gamma\} \qquad \text{as } \nu r\rightarrow 0 \quad (2.84)$$

where γ is Euler's constant, the diagonal coefficients are given as

$$a_{ii} = \frac{\nu}{\pi} K_1[2\nu(z_i+d)]\Delta x_i \qquad (2.85)$$

$$b_{ii} = \frac{\Delta S_i}{\pi}[\ln\frac{\nu\Delta S_i}{4} + \gamma - 1 - K_0\{2\nu(z_i+d)\}] \qquad (2.86)$$

For $\beta=0°$, the problem reduces to the typical two dimensional one. Using the Green's function given in eqn. (2.27) with symmetry about the seabed taken into account, the coefficients for $\beta=0°$ are given by

$$a_{ij} = -\frac{1}{\pi r_{ij}^2}[(x_j-x_i)\Delta z_j - (z_j-z_i)\Delta x_j] -$$

$$\frac{1}{\pi r_{ij}'^2}[(x_j-x_i)\Delta z_j - (z_j+2d+z_i)\Delta x_j] \quad i\neq j \qquad (2.87)$$

$$b_{ij} = \frac{1}{\pi}(\ln r_{ij} + \ln r'_{ij})\Delta S_j \qquad i\neq j \qquad (2.88)$$

For i=j

$$a_{ii} = \frac{\Delta x_i}{2\pi(z_i+d)} \qquad (2.89)$$

$$b_{ii} = \frac{\Delta S_i}{\pi}[\ln\frac{\Delta S_i}{2} - 1 + \ln 2(z_i+d)] \qquad (2.90)$$

With the coefficients a_{ij} and b_{ij} now known, eqn. (2.70) provides N equations relating the values of ϕ and $\partial\phi/\partial n$ over $S_B+S_F+S_R$. The various boundary conditions around $S_B+S_F+S_R$ provide the remaining N equations needed to solve for ϕ and $\partial\phi/\partial n$. Substitution of the various boundary conditions given in eqn. (2.15) into eqn. (2.70) yields

$$\sum_{j=1}^{N1}(a_{ij}+\delta_{ij}+\frac{\omega^2 a}{g}b_{ij})\phi_j^{(k)} + \sum_{j=N1+1}^{N2}(a_{ij}+\delta_{ij})\phi_j^{(k)} +$$

$$\sum_{j=N2+1}^{N3}(a_{ij}+\delta_{ij}+\frac{\omega^2 a}{g}b_{ij})\phi_j^{(k)} + \sum_{j=N3+1}^{N4}(a_{ij}+\delta_{ij}+ik\cos\beta b_{ij})\phi_j^{(k)} +$$

$$\sum_{j=N4+1}^{N}(a_{ij}+\delta_{ij}+ik\cos\beta b_{ij})\phi_j^{(k)} = -\sum_{j=N1+1}^{N2} b_{ij}f_j^{(k)}$$

$$\text{for } i=1,\ldots,N;\ k=1,2,3,4 \qquad (2.91)$$

where $f_j^{(k)}$ is defined as

$$f_j^{(k)} = \begin{cases} n_j^{(k)} & k=1,2,3 \\ -\dfrac{\partial \phi_j^{(4)}}{\partial n} & k=4 \end{cases} \tag{2.92}$$

The expressions on the right-hand side of the above equation are given as

$$\frac{\partial \phi_j^{(4)}}{\partial n} = ik\cos\beta \frac{\cosh[k(z_j+d)]}{\cosh(kd)} \exp(ik\cos\beta x_j)\frac{\Delta z_j}{\Delta S_j} - k\frac{\sinh[k(z_j+d)]}{\cosh(kd)} \exp(ik\cos\beta x_j)\frac{\Delta x_j}{\Delta S_j} \tag{2.93}$$

and

$$n_j^{(k)} = \begin{cases} \Delta z_j/\Delta S_j & k=1 \\ -\Delta x_j/\Delta S_j & k=2 \\ (z_j-e)\dfrac{\Delta z_j}{\Delta S_j} + x_j\dfrac{\Delta x_j}{\Delta S_j} & k=3 \end{cases} \tag{2.94}$$

Fig. 5 shows a typical discretized boundary with the constants N1, N2, N3 and N4 shown. Eqn. (2.91) yields N equations for N unknown $\phi_j^{(k)}$ (k=1,2,3,4) values which can be solved using a matrix inversion technique to obtain the unknown velocity potentials on the boundary. The exciting forces, added mass and damping coefficients, and reflection and transmission coefficients can now be determined using the expressions given in the preceding sections.

2.8 EFFECT OF FINITE STRUCTURE LENGTH

Let us now consider the forces and response of a rigid structure of finite length, l. The length of the structure is assumed to be much greater than the incident wavelength.

The force per unit length is given by eqn. (2.32) as

$$F_j(y,t) = \rho g \frac{H}{2} \begin{Bmatrix} a \\ a_2 \end{Bmatrix} \mathrm{Re}[C_j(\omega,\beta)\exp\{i(\nu y-\omega t)\}] \quad \begin{Bmatrix} j=1,2 \\ j=3 \end{Bmatrix} \tag{2.95}$$

where j=1,2,3 corresponds to the sway, heave and roll exciting forces (or moment). The total force on the structure is obtained by integrating two-dimensional force along its length, ignoring end effects

$$F_j(t) = \int_{-l/2}^{l/2} F_j(y,t)dy \tag{2.96a}$$

Substitution of eqn. (2.95) into eqn. (2.96a) yields

$$F_j(t) = \rho g \frac{H}{2} l \begin{Bmatrix} a \\ a_2 \end{Bmatrix} C_j \frac{2\sin(\frac{kl}{2}\sin\beta)}{kl\sin\beta} \exp(-i\omega t) \begin{Bmatrix} j=1,2 \\ j=3 \end{Bmatrix} \tag{2.96b}$$

for $\beta \neq 0°$. The above expression can be thought of as the product of the force per unit length, the length of the structure, and a factor $r(kl,\beta)$ defined as

$$r(kl,\beta) = \begin{cases} \dfrac{2\sin(\frac{kl}{2}\sin\beta)}{kl\sin\beta} & \beta \neq 0° \\ 1 & \beta = 0° \end{cases} \tag{2.97}$$

The factor $r(kl,\beta)$ can be considered to be a reduction of the load per unit length due to the finite length of the structure for a given angle of approach, or due to the obliqueness of the waves for a given structure length. Fig. 6 shows a plot of r^2 against kl for $\beta=0°$, 15°, 30° and 60°. The separate influences of kl and β on the load per unit length can be seen. The factor $r(kl,\beta)$ has an oscillatory behavior at large values of kl with an infinite number of zeros given by

$$\frac{kl}{2}\sin\beta = n\pi \qquad n=1,2,... \tag{2.98}$$

For an infinite span structure, the total load per unit length tends to zero. The maximum total load occurs on a span of length

$$l = L/2\sin\beta \tag{2.99}$$

where $L=2\pi/k$ is the wavelength. This maximum force is

$$F_j(t) = \rho g\frac{H}{2}\begin{Bmatrix}a\\a_2\end{Bmatrix}C_j(\omega,\beta)\frac{2}{k\sin\beta}\exp(-i\omega t)\quad\begin{Bmatrix}j=1,2\\j=3\end{Bmatrix} \tag{2.100}$$

The motions of a rigid cylinder of finite length in oblique seas can be described in terms of six degrees of freedom. In addition to the sway, heave and roll modes present in beam seas, the cylinder can also surge, yaw and pitch corresponding to the translational motion along the y axis and rotational motions about the z and x axes respectively.

The added mass and damping coefficient derived in section 2.4 corresponds to the oscillations of a flexible cylinder with a sinusoidal variation of the amplitude of motion along the length of the cylinder. The added mass and damping coefficients of a rigid cylinder correspond to the case of beam seas ($\beta=0°$). The hydrodynamic coefficients for the sway, heave and roll motions of a finite length structure are obtained by multiplying the sectional coefficients with the length of the structure. The exciting forces and hydrodynamic coefficients for the pitch and yaw motions can be obtained from the sectional coefficients for the heave and sway motions using a strip theory approach

described in Bhattacharyya (1978). The yaw and pitch exciting exciting moment coefficients are given as

$$F_{j+3}(t) = \int_{-l/2}^{l/2} yF_j(y,t)dy \qquad j=1,2 \quad (2.101)$$

where j=4,5 corresponds to the yaw and pitch modes respectively. Substitution of expression for the two-dimensional forces (2.95) into eqn. (2.101) yields

$$F_{j+3}(t) = \rho g \frac{H}{2} a l^2 C_j \cdot q(kl,\beta)\exp(-i\omega t) \quad j=1,2 \quad (2.102)$$

where $q(kl,\beta)$ is defined as

$$q = \begin{cases} \frac{2i}{(kl\sin\beta)^2}\left[\frac{kl}{2}\sin\beta\cos\left(\frac{kl}{2}\sin\beta\right) - \sin\left(\frac{kl}{2}\sin\beta\right)\right] & \beta \neq 0° \\ 0 & \beta = 0° \end{cases} \quad (2.103)$$

3. EFFECTS OF DIRECTIONAL WAVES

3.1 REPRESENTATION OF DIRECTIONAL SEAS

Before proceeding to determine the response of structures in directional seas, we shall first present a mathematical representation of directional seas.

The preceding chapter dealt with the exciting forces and response of a structure subject to regular unidirectional waves. Ocean waves however exhibit a wave pattern which is highly complex and irregular. This complex sea surface is often modelled by a linear superposition of long-crested waves of all possible frequencies approaching a point from all directions. The sea surface elevation is assumed to be a zero mean, stationary, ergodic random Gaussian process. The assumption of a Gaussian process implies symmetry about the still water level which is only realistic for small amplitude waves.

A long-crested wave train travelling at angle β relative to the positive x axis may be represented by

$$\eta(x,y,t) = \mathrm{Re}[A \exp\{i(kx\cos\beta+ky\sin\beta-\omega t)\}] \qquad (3.1)$$

where A is the complex wave amplitude with a random phase, k is the wave number related to the frequency ω by the linear dispersion relation (eqn. 2.11).

A random sea surface can be considered to be a discrete sum of linear waves of different frequencies and directions

$$\eta = \mathrm{Re}[\sum_{ij}\sum A_{ij}\exp\{i(k_i x\cos\beta_j+k_i y\sin\beta_j-\omega_i t)\}] \qquad (3.2)$$

where k_i denotes the wave number of the i-th wave component travelling in direction β_j, ω_i its frequency and A_{ij} its amplitude. If we let the total number of harmonics tend to infinity while the difference between adjacent frequencies and directions tends to zero, the summation in eqn. (3.2) can be replaced by an integral over a continuous range of frequencies and directions

$$\eta(x,y,t) = \mathrm{Re}[\int\int \exp\{i(kx\cos\beta+ky\sin\beta-\omega t)\}dA(\omega,\beta)] \qquad (3.3)$$

where dA represents the differential wave amplitude in the two-dimensional (ω,β) space bounded by $(\omega,\omega+d\omega)$ and $(\beta,\beta+d\beta)$. The mean square value of the water surface elevation is given by

$$\overline{\eta^2} = \frac{1}{2}\int\int dA(\omega,\beta)dA^*(\omega,\beta) = \int_{-\pi}^{\pi}\int_{0}^{\infty} S(\omega,\beta)d\omega d\beta \qquad (3.4)$$

where $dA^*(\omega,\beta)$ is the complex conjugate of $dA(\omega,\beta)$ and $S(\omega,\beta)$ is a directional wave spectrum. Since the average energy density in the waves is proportional to the square of the wave amplitude, the product $S(\omega,\beta)d\omega d\beta$ can be considered to be the contribution to the total mean energy density due to waves with frequencies between ω and $\omega+d\omega$, travelling in directions between β and $\beta+d\beta$. A sketch of a typical directional wave spectrum is shown in Fig. 7.

The one-dimensional spectrum, $S(\omega)$ can be obtained by integrating the directional wave spectrum over all directions

$$S(\omega) = \int_{-\pi}^{\pi} S(\omega,\beta)d\beta \qquad (3.5)$$

The one-dimensional wave spectrum can be determined from measurements of the free surface elevation at a single point in space; for instance by recording the motions of a heaving buoy. In order to obtain information about the directionality of the waves, one has to resort to more complicated techniques. The most common methods for evaluating directional wave spectra include

1. analysis of the water surface elevation and the horizontal orbital velocities at an observation point (e.g. Forristall et al (1978), Sand (1980)).
2. analysis of the measurements of the water surface elevation, slope and curvature from the motions of a floating buoy (e.g. Longuet-Higgins *et al* (1961), Cartwright and Smith (1964), Mitsuyasu *et al* (1975)).
3. analysis of the measurements of the water surface elevation from an array of guages (e.g. Borgman (1969), Panicker (1971), Davis and Regier (1977)).
4. by means of stereophotographs (e.g. Coté *et al* (1960), Holthujsen (1981)).

It is often convenient to express the directional wave spectrum in terms of an energy spreading function applied to the one-dimensional spectrum

$$S(\omega,\beta) = S(\omega)G(\omega,\beta) \qquad (3.6)$$

where $G(\omega,\beta)$ is a directional spreading function.

It follows from eqn. (3.5) that $G(\omega,\beta)$ must satisfy

$$\int_{-\pi}^{\pi} G(\omega,\beta)d\beta = 1 \tag{3.7}$$

Various one-dimensional frequency spectra have been used describe ocean waves. The most commonly used ones include the Bretschneider, Pierson-Moskowitz and JONSWAP spectra. These spectra are described in detail in Sarpkaya and Isaacson (1981) and hence are not given here. There have also been several formulations for $G(\omega,\beta)$ proposed by various authors. A few of the commonly used ones are outlined below

1. Cosine-squared formulation

St. Denis and Pierson (1953) proposed a spreading function which is independent of frequency

$$G(\beta) = \begin{cases} \frac{2}{\pi}\cos^2\beta & \text{for } |\beta| < \pi/2 \\ 0 & \text{otherwise} \end{cases} \tag{3.8}$$

The spectrum is centred about $\beta=0°$.

2. Cosine-power formulation

Longuet-Higgins *et al* (1961) proposed the following directional spreading function

$$G(\theta) = C(s)\cos^{2s}(\theta) \tag{3.9}$$

where θ is measured from the principal direction of wave propagation. C(s) is a normalizing coefficient that ensures that eqn. (3.7) is satisfied and is given by

$$C(s) = \frac{1}{2\sqrt{\pi}} \frac{\Gamma(s+1)}{\Gamma(s+\frac{1}{2})} \tag{3.10}$$

Γ is the gamma function. Fig. 8 shows the directional spreading function for different values of s. It can be seen that s describes the degree of spread about the principal direction with $s \to \infty$ representing long-crested waves.

On the basis of their measurements for wind driven ocean waves, Mitsuyasu *et al* (1975) found the parameter s to depend on the dimensionless frequency

$$s = \begin{cases} 0.116(\bar{f})^{-2.5} & \text{for } \bar{f} \geq \bar{f}_m \\ 0.116(\bar{f})^{-5}(\bar{f}_m)^{-7.5} & \text{for } \bar{f} < \bar{f}_m \end{cases} \tag{3.11}$$

where $\bar{f}$ = dimensionless frequency = Uf/g

$\bar{f}_m$ = dimensionless modal frequency = Uf_m/g

U = wind speed at 19.5m above sea level

Hasselmann *et al* (1980) on the basis of the data obtained from the Joint North Sea Wave Project (JONSWAP) found the parameter s to depend mainly on f/f_m rather than $\bar{f}$ and proposed a different formula for s.

Borgman (1969) used an alternative cosine power function given as

$$G(\theta) = \begin{cases} C'(s) \cos^{2s}(\theta) & \text{for } |\theta| < \pi/2 \\ 0 & \text{otherwise} \end{cases} \tag{3.12}$$

The normalizing coefficient C'(s) is given as

$$C'(s) = \frac{1}{\sqrt{\pi}} \frac{\Gamma(s+1)}{\Gamma(s+\frac{1}{2})} \tag{3.13}$$

3. SWOP formulation

Coté *et al* (1960) proposed a directional spreading function which is dependent on both frequency and direction based on data obtained from the Stereo Wave Observation Project (SWOP).

$$G(\omega,\theta) = \begin{cases} \frac{1}{\pi}[1 + a\cos 2\theta + b\cos 4\theta] & \text{for } |\theta| < \pi/2 \\ 0 & \text{otherwise} \end{cases} \qquad (3.14)$$

where $a = 0.50 + 0.82\exp(-\frac{1}{2}\bar{\omega}^4)$

$b = 0.32\exp(-\frac{1}{2}\bar{\omega}^4)$

$\bar{\omega}$ = nondimensional frequency = $U\omega/g$

3.2 RESPONSE TO DIRECTIONAL WAVES

The exciting force on a rigid structure of finite length due to a regular oblique wave train of frequency ω and direction β can be expressed as

$$F_j(t) = H_j(\omega,\beta)\eta(t) \qquad (3.15)$$

where $H_j(\omega,\beta)$ is a complex-valued system response function given by eqn. (2.96b) as

$$H_j(\omega,\beta) = \rho g l \begin{Bmatrix} a \\ a^2 \end{Bmatrix} C_j(\omega,\beta) r(kl,\beta) \qquad \begin{Bmatrix} j=1,2 \\ j=3 \end{Bmatrix} \qquad (3.16)$$

Since the wave-structure interaction process is assumed linear, we expect the value of any force at a given wave frequency to be due to wave components at that same frequency but propagating from all possible directions. The force spectrum $S_{F_j}(\omega)$ is thus related to the incident wave spectrum $S_\eta(\omega,\theta)$ by

$$S_{F_j}(\omega) = \int_{-\pi}^{\pi} |H_j(\omega,\beta)|^2 S_\eta(\omega,\theta)d\beta \qquad (3.17)$$

where $|H_j(\omega,\beta)|^2$ is the transfer function. For convenience, the subscript j will henceforth be dropped and it should be noted that all following expressions are valid for j=1,2,3. Since the water surface elevation is assumed to be a Gaussian process, the forces will possess a Gaussian probability distribution.

Using the form of the directional wave spectrum given in eqn. (3.6), eqn. (3.17) reduces to

$$S_F(\omega) = \left[\int_{-\pi}^{\pi} |H(\omega,\beta)|^2 G(\omega,\theta)d\beta\right] S_\eta(\omega) \qquad (3.18)$$

The factor in the brackets represents a frequency dependent, directionally averaged transfer function. θ is measured from the principal wave direction β_o and is thus related to β by

$$\theta = \beta - \beta_o \qquad (3.19)$$

The mean square value of the force can be obtained by integrating the force spectrum over the frequency ω. The root mean square value (rms) of the force represents a characteristic force from which extreme value predictions are usually made.

The effects of wave directionality on the wave loads can be expressed as a force reduction factor defined as the ratio of the frequency dependent, directionally averaged transfer function in short-crested seas to the transfer function for long-crested, normally incident waves

$$R_F^2 = \frac{\int_{-\pi}^{\pi} |H(\omega,\beta)|^2 G(\omega,\theta)\,d\beta}{|H(\omega,0)|^2} \tag{3.20}$$

A body response ratio R_M can also defined as the ratio of the rms value of the response in short-crested seas to corresponding results for long-crested seas, that is

$$R_M^2 = \frac{\int_0^{\infty}\int_{-\pi}^{\pi} |Z(\omega,\beta)|^2 G(\omega,\theta) S_\eta(\omega)\,d\beta\,d\omega}{\int_0^{\infty} |Z(\omega,0)|^2 S_\eta(\omega)\,d\omega} \tag{3.21}$$

where $Z(\omega,\beta)$ is the response amplitude operator defined previously in eqn. (2.56).

The first example considered is the wave force on an infinitesimal segment of a structure with the sinusoidal variation along the length neglected. The horizontal force at any angle β is proportional to $\cos\beta$. The transfer function can thus be expressed as

$$|H(\omega,\beta)|^2 = |H(\omega,0)|^2 \cos^2\beta \tag{3.22}$$

The frequency independent cosine-power directional spreading function given in eqn. (3.12) is used in this study. Substitution of the expressions for the transfer function (3.22) and spreading function (3.12) into eqn. (3.20) yields

$$R_F^2 = C'(s) \int_{-\pi/2}^{\pi/2} \cos^2\beta \cos^{2s}(\theta)\,d\theta \tag{3.23}$$

For the case of oblique mean incidence, the directional distribution will be cut off to ensure that the waves approach the structure from one side only. If the principal

direction of wave propagation is zero, eqn. (3.23) can be integrated to give

$$R_F^2 = \frac{C'(s)}{C'(s+1)} \tag{3.24}$$

For any given structure of arbitrary shape and finite length, the dependence on β is no longer explicit and eqn. (3.20) will have to be integrated numerically to give the force reduction factor. Substitution of the expression for the transfer function (3.16) into eqn. (3.20) yields

$$R_{F_j}^2 = C'(s)\frac{\int_{-\pi/2}^{\pi/2} |C_j(\omega,\beta)|^2 r^2(kl,\beta)\cos^{2s}(\theta)d\theta}{|C_j(\omega,0)|^2} \tag{3.25}$$

for the cosine-power type spreading function.

4. RESULTS AND DISCUSSION

4.1 EXCITING FORCES, ADDED MASS AND DAMPING COEFFICIENTS

A computer program based on the procedure described in the preceding sections was used to determine the exciting forces, hydrodynamic coefficients, and reflection and transmission coefficients for several test cases in order to compare the accuracy and efficiency of the present method with other solution techniques.

The first case considered is a rectangular section cylinder with a draft to half-beam (b/a) ratio of 1, in water of finite depth (d/a=2). Figs. 9-12 show a comparison of the computed exciting force and reflection coefficients with the results obtained by Bai (1975) using a finite element technique. The coefficients are plotted as a function of the angle of incidence β for ka=0.1, 0.2 and 0.4. Bai's (1975) results are represented by the solid and dashed curves while the present results are shown as points.

The discretized surface had 40 node points on the free surface, 20 node points on the radiation surface and 16 node points on the body surface yielding a matrix of dimension N=76. It took approximately 3.0s on the Amdahl V8-II central processor under the Michigan Terminal System (MTS) to solve for the exciting force coefficients for a given wavenumber and angle of incidence. Bai (1975) used an 88 element, 325 node finite element mesh with a CPU time of 12s on an IBM 370 computer. The present procedure is thus relatively quite

efficient.

The computed sway and heave exciting force coefficients and the reflection coefficient agree quite closely with Bai's (1975) results. The roll exciting moment coefficient was consistently greater than that presented by Bai (1975) with a maximum difference of about 7.5%. The use of a much larger set of node points did not significantly change the present results. The difference is expected to diminish with the use of a finer mesh in Bai's computations.

From Figs. 9-11 it can be seen that the exciting force coefficients decrease with increasing angle of incidence vanishing at $\beta=90°$. The maximum force or moment occurs at $\beta=0°$. The heave exciting force coefficient was fairly constant up to certain angle before decreasing to zero at $\beta=90°$, while the sway and roll exciting force (or moment) coefficients at any angle β seemed to be proportional to $\cos\beta$ for ka=0.1. The reflection coefficient decreases slightly with increasing angle of incidence before increasing to one at $\beta=90°$.

The exciting force and hydrodynamic coefficients of a rectangular cylinder with a draft of 0.265a in water of infinite depth were also computed and compared with the results of Garrison (1984) in Figs. 13-21. Garrison (1984) used a Green's function which satisfies the free surface and radiation boundary conditions and thus requires the discretization of the cylinder surface only. The Green's function used in the present procedure is relatively simple

while the Green's function used by Garrison (1984) is quite complex and is only valid for water of infinite depth. A water depth $d=\pi/k+b$, where k is the wavenumber is used in the present procedure to simulate infinite water depth. The discretized surface had 40 node points on the free surface, 40 node points on the radiation surface and 16 node points on the body surface. The coefficients are plotted as a function of the frequency parameter ka for angles of incidence $\beta=0°$, 30° and 60°. The computed exciting force coefficients agree quite well with Garrision's (1984) results. The added mass and damping coefficients generally show good agreement with Garrison's results. The sway added mass coefficient at 60° deviated by as much as 15% while the roll damping coefficients deviated substantially from Garrison's results with differences of up to 25%. Garrison's results however agreed much better with the Haskind relations. The results were slightly sensitive to the location of the radiation distance which was estimated empirically. The use of elements with higher order variations of the potential should improve the accuracy of the present method.

The exciting force coefficients show the expected tendencies, decreasing with increasing angle of incidence. The maximum roll moment occurs at about $ka=\pi/4$. This result agrees with intuition since one would expect the maximum moment to occur when the trough of a wave is at the origin and the crest at the sides of the cylinder.

The added mass coefficients tended to increase, while the damping coefficient decreased with increasing angle of incidence for most of the frequency range studied. The damping coefficients should vanish at $\beta=90°$ since the wave crests are normal to the axis of the cylinder and hence no energy is propagated away from the cylinder in the $\pm x$ directions.

The exciting force coefficients, hydrodynamic coefficients and wave amplitude ratios of a semi-immersed circular cylinder in water of infinite depth were computed and are compared with the results of Bolton and Ursell (1973), and Garrison (1984) in Tables 1-4. Garrison's results were estimated from the figures presented in his paper. The results are shown for ka=0.25, 0.75 and 1.25 with angles of incidence $\beta=0°$, 35° and 55°. The boundary was modelled with 40 node points on the free surface, 40 node points on the radiation surface and 16 straight line segments on the surface of the cylinder. Agreement between the different methods is generally good with differences of less than 15%. It is interesting to note that the wave amplitude ratios increase with angle of incidence. This indicates that as the wavelength along the cylinder decreases, the waves generated by the motions of the cylinder become more amplified.

4.2 MOTIONS OF AN UNRESTRAINED BODY

The equations of motion were solved to give the amplitudes of motion of a long floating box (a=7.5m, b=3m, l=75m) in water of depth d=12m. The box is assumed to be rigid and hence the added mass and damping coefficients for beam seas (β=0°) are used. The mass of the box is ρV where V is the displaced volume. The centre of gravity is assumed to be at the still water level and the roll radius of gyration is given as 19.5m.

Figs. 22-24 show the amplitudes of motion for the sway, heave and roll modes respectively. The amplitudes are plotted as a function of ka for β=0°, 30° and 60°. At low frequencies (ka≤0.1), the sway and heave motions have the same amplitudes as the horizontal and vertical motions of a particle at the free surface. The sway amplitude is maximum as ka→0 and decreases as ka increases. The heave amplitude for beam seas increases with ka up to maximum before decreasing, while the response amplitudes for β=30° and 60° decrease with increasing ka. There are local zeros of the response for oblique waves corresponding to the zeros of the factor r(kl,β). The roll amplitude at resonance is excessively high. This is because viscous damping which is present in practical situations was neglected in the computations. In solving the equations of motion, it was observed that the heave response is uncoupled from the sway and roll responses while coupling between the sway and roll modes was weak except close to the roll resonance frequency

where there is a sudden drop in the sway amplitude.

4.3 EFFECTS OF DIRECTIONAL WAVES

There are two factors that contribute to the reduction of wave loads experienced by long structures in short-crested seas compared to long-crested seas: (1) the sinusoidal variation of the wave forces along the length of the structure, and (2) the variation of the two-dimensional forces with angle of incidence for a given cross-section.

The integration of the two-dimensional force along the length of the structure results in a reduction factor $r(kl,\beta)$. The square of the reduction factor $r(kl,\beta)$ is plotted as a function of kl for β=0°, 15°, 30° and 60° in Fig. 6. For a given structure of finite length, the factor $r(kl,\beta)$ results in the reduction of the wave loads per unit length for oblique waves even if there is no variation of the sectional force with angle of incidence. It also results in the decrease of the wave loads per unit length as ka increases if we ignore the variation of the sectional forces with ka. The variation of the sectional forces with the frequency parameter ka and angle of incidence β has been discussed previously in section 4.1. The combination of the factor $r(kl,\beta)$ with the sectional force variation with angle of incidence results in the total force reduction factor R_F.

The frequency dependent force reduction factor R_F has been computed for the long floating box described in section 4.2. The computed R_F values for the cosine power type energy

spreading function is plotted as a function of ka in Figs. 25(a)-(c) for the sway, heave and roll forces (or moment) respectively. The results are shown for s=1,3,6 in order to assess the influence of the degree of wave short-crestedness. A principal direction $\beta_0=0°$ was used in the computations. Simpson's rule was used to carry out the numerical integration in eqn. (3.25) with an interval of 10°.

At low frequencies, the heave force reduction factor approaches a limiting value of one. This confirms the fact that the heave exciting force is independent of direction for low values of ka. As ka (or kl) increases, there is a significant reduction of the heave force mostly due to the factor $r(kl,\beta)$. The sinusoidal variation along the length thus makes it important to account for directional spreading particularly for long structures. It can also be seen from Figs. 25(a)-(c) that as s increases, the forces approach the results for long-crested seas. Battjes (1982) derived an expression for the asymptotic form of R_F at high frequencies. This is given as

$$R_F^2 = 2\pi C(s)\cos^{2s}\beta_0/kl \qquad \text{as } kl\to\infty \qquad (4.1)$$

At higher frequencies (ka>1), the sway, heave and roll force (or moment) reduction factors all converge to a value which is slightly less than the asymptotic value. The sway and roll force (or moment) reduction factors approach a value of 0.866 as ka→0. This result was expected since the sectional

sway and roll exciting force (or moment) is proportional to $\cos\beta$ at low frequencies ($ka<0.1$). The force reduction factors for all three modes decrease with increasing ka up to a value of 0.4 at ka=2.

The sway and heave force reduction factors were also computed for one case of oblique mean incidence ($\beta_0=30°$) and the results are shown in Figs. 26(a)-(b). The reduction factors for normal mean incidence are included for comparison. At low frequencies, the sway force reduction factor has a value of 0.79 for $\beta_0=30°$ compared to 0.866 for normal mean incidence. The heave force reduction factor at ka=0 was 0.985 for $\beta_0=30°$ compared to 1.0 for $\beta_0=0°$. The slight reduction of the heave force arises from the fact that the spreading function was cut off to ensure that the waves approach the structure from one side only. As ka increases, the difference between the heave force reduction factor for oblique mean waves and normal mean waves increases up to an asymptotic ratio of $\cos\beta_0$.

The response ratio for the body motions has been computed for the case of the floating box subject to a Bretschneider spectrum with cosine power energy spreading. The incident unidirectional wave spectrum is given as

$$S(\omega) = \frac{5H_s^2}{16f_0} \frac{1}{(f/f_0)^5} \exp[-\frac{5}{4}(\frac{f}{f_0})^{-4}] \qquad (4.2)$$

where H_s is the significant wave height and f_0 is the peak frequency. The results are plotted as a function of s in Figs. 27(a)-(c) for the sway, heave and roll responses

respectively assuming normal mean incidence. A significant wave height H_s=2m and a peak frequency f_0=0.2Hz were used in the computations. In the numerical integration, five frequencies between 0.14Hz and 0.26Hz and an angle interval of 10° were used. The rms amplitudes in long-crested seas are 0.22m, 0.32m and 0.60rad for the sway, heave and roll responses respectively. Figs. 27(a)-(c) show reductions of 43%, 42.5% and 41.5% in the rms value of the sway, heave and roll responses respectively in short-crested seas with s=1 compared to long-crested seas. As s increases, the response ratios approach a limiting value of one indicating that the amplitudes of motion of the structure in short-crested seas approach the long-crested results as $s\rightarrow\infty$.

5. CONCLUSIONS AND RECOMMENDATIONS

5.1 CONCLUSIONS

The effects of wave directionality on the loads and motions of long structures has been studied.

A numerical method based on Green's theorem has been developed to compute the exciting forces and hydrodynamic coefficients associated with the interaction of a regular oblique wave train with an infinitely long, floating semi-immersed cylinder of arbitrary shape. The method is quite general and can be applied to cases of variable water depth.

Numerical results obtained from the present method have been compared with those obtained by Bai (1975) using a finite element method for a rectangular section cylinder in water of finite depth. The present results have also been compared to those obtained for infinite water depth by Bolton and Ursell (1973) using a multipole method for a semi-immersed circular cylinder as well as Garrison (1984) using a Green's function procedure for a rectangular cylinder and a semi-immersed circular cylinder.

The present method is quite efficient and gives results which compare favorably with all the previous results over a wide range of frequencies covering the usual range of design conditions. The present procedure is not as efficient for very high frequencies due to the large number of node points required to give accurate results. The present procedure is

however not valid for head seas since the wavelength along the body axis becomes of the same order of magnitude as a typical cross-sectional dimension.

The two-dimensional results have been integrated along the body axis to obtain the wave loads on structures of finite length. The wave loads and motions of a rigid structure in short-crested seas have been obtained using the linear transfer function approach. The effects of wave directionality is expressed as a frequency dependent, directionally averaged reduction factor for the wave loads and a response ratio for the body motions. The reduction factors have been evaluated numerically for the cosine-power type directional spreading function. Response ratios were also computed for a Bretschneider incident wave spectrum with cosine power spreading.

For the given structure, the sway and roll force reduction factors varied from 0.87 at ka=0 to 0.41 at ka=2 for a cosine-squared distribution with normal mean incidence. The heave reduction factor varied from 1.0 at ka=0 to 0.40 at ka=2. The ratio of the amplitudes of motion of the structure for the specified short-crested sea state with a cosine-squared distribution were 57%, 57.5% and 58.5% of the response in long-crested seas for the sway, heave and roll modes respectively. A further reduction of the forces and amplitudes of motions is obtained for oblique mean waves ($\beta_0 \neq 0°$). These reductions are quite significant particularly for long relative structure lengths and need to be

considered in the design process.

As the parameter s which describes the degree of short-crestedness increases, the loads and motions in short-crested seas approach the results for long-crested seas.

5.2 RECOMMENDATIONS FOR FURTHER STUDY

There are several areas in which further studies could be made to improve the present method. The accuracy of the numerical scheme used in the solution of the oblique wave diffraction problem could be improved by using higher order elements. This however requires an increased computing effort.

The present study considered the effects of wave directionality on the loads and motions of a rigid body even though hydrodynamic coefficients have been presented for structures with sinusoidal mode shapes. A numerical procedure could be developed to determine the dynamic response of a flexible structure such as a floating bridge in short-crested seas using the exciting forces and hydrodynamic coefficients given by the present method. Additional forces due to moorings and viscous damping could be included in the analysis.

The present method assumes a small amplitude wave train. For steep waves, nonlinear effects have to be considered. Developing a theory that incorporates both the nonlinearity and directionality of the waves is however

quite difficult. The present linear diffraction theory for oblique waves could be extended to nonlinear waves and a hybrid method such as that proposed by Dean (1977) can be used to include the effects of wave directionality.

Finally, experimental investigations could be carried out to measure the loads and response of long structures in short-crested seas to help verify the present theoretical results.

BIBLIOGRAPHY

1. Abramowitz, M. and Stegun, I.A. 1964. *Handbook of Mathematical Functions*. Dover Publications, New York.

2. Bai, K.J. 1972. A variational method in potential flows with a free surface. Report No. NA72-2, College of Engineering, University of California, Berkeley.

3. Bai, K.J. 1975. Diffraction of oblique waves by an infinite cylinder. *J. Fluid Mech.* **68**, pp. 513-535.

4. Battjes, J.A. 1982. Effects of short-crestedness on wave loads on long structures. *Applied Ocean Research.* **4**(3), pp. 165-172.

5. Bearman, P.W., Graham, J.M.R., and Singh, S. 1979. Forces on cylinders in harmonically oscillating flow. In *Mechanics of Wave Induced Forces on Cylinders*, ed. T.L. Shaw, Pitman, London, pp. 437-449.

6. Bhattacharyya, R. 1978. *Dynamics of Marine Vehicles.* John Wiley and Sons, New York.

7. Black, J.L. and Mei, C.C. 1970. Scattering and radiation of water waves. Rep. No. 121, Water Resources and Hydrodynamics Laboratory, Dept. of Civil Engineering, Massachusetts Institute of Technology.

8. Bolton, W.E. and Ursell, F. 1973. The wave force on an infinitely long cylinder in an oblique sea. *J. Fluid Mech.* **57**, pp. 241-256.

9. Borgman, L.E. 1969. Directional spectra models for design use. *Proc. Offshore Tech. Conf.*, Houston, Paper No. OTC1069, pp. 721-746.

10. Bryden, I.G. and Greated, C.A. 1984. Hydrodynamic response of long structures to random seas. *Proc. Symp. on Description and Modelling of Directional Seas*, Copenhagen.

11. Cartwright, D.E. and Smith, N.D. 1964. Buoy techniques for obtaining directional wave spectra. *Buoy Technol., Mar. Technol. Soc.*, pp. 173-182.

12. Coté, L.J. *et al.* 1960. The directional spectrum of a wind generated sea as determined from data obtained by the Stereo Wave Observation Project. *Meteorological Paper*, **2**(6), College of Engineering, New York University.

13. Dallinga, R.P., Aalbers, A.B., and van der Vegt, J.W.W.

1984. Design aspects for transport of jack-up platforms on a barge. *Proc. Offshore Tech. Conf.*, Houston, Paper No. OTC4733, pp. 195-202.

14. Davis, R.E. and Regier, L.A. 1977. Methods for estimating directional wave spectra from multi-element arrays. *J. Marine Research.* **35**(3), pp. 453-477.

15. Dean, R.G. 1977. Hybrid method of computing wave loading. *Proc. Offshore Tech. Conf.*, Houston, Paper No. OTC3029, pp. 483-492.

16. Finnigan, T.D. and Yamamoto, T. 1979. Analysis of semi-submerged porous breakwaters. *Proc. Civil Engineering in the Oceans IV,* ASCE, San Fransisco, pp. 380-397.

17. Forristall, G.Z., Ward, E.G., Cardone, V.J., and Borgman, L.E. 1978. The directional spectra and kinematics of surface gravity waves in tropical storm Delia. *J. Phys. Oceanography.* 8, pp. 888-909.

18. Garrison, C.J. 1969. On the interaction of an infinite shallow-draft cylinder oscillating at the free surface with a train of oblique waves. *J. Fluid Mech.* **39**, pp. 227-255.

19. Garrison, C.J. 1984. Interaction of oblique waves with an infinite cylinder. *Applied Ocean Research.* **6**(1), pp. 4-15.

20. Georgiadis, C. 1984. Time and frequency domain analysis of marine structures in short-crested sea by simulating appropriate nodal loads. *Proc. 3rd Int. Symp. on Offshore Mechanics and Arctic Engineering,* New Orleans, pp. 177-183.

21. Hackley, M.B. 1979. Wave force simulations in random directional seas. *Proc. 2nd Int. Conf. on the Behaviour of Offshore Structures, BOSS'79,* London, pp. 187-219.

22. Haskind, M.D. 1953. *Oscillation of a ship in a calm sea.* English translation, Soc. of Naval Architects and Marine Engineers, T&R Bulletin 1-12.

23. Hasselmann, K., Dunckel, M., and Ewing, J.A. 1980. Directional wave spectra observed during JONSWAP. *J. Phys. Oceanography.* **10**, pp. 1264-1280.

24. Holthujsen, L.H. 1981. The directional energy distribution of wind generated waves as inferred from stereophotographic observations of the sea surface. Rep. No. 81-2, Dept. of Civil Engineering, Delft Univ. of Technology.

25. Huntington, S.W. and Thompson, D.M. 1976. Forces on a large vertical cylinder in multi-directional random waves. *Proc. Offshore Tech. Conf.*, Houston, Paper No. OTC2539, pp. 169-183.

26. Ijima, T., Chou, C.R., and Yoshida, A. 1976. Method of analysis for two-dimensional water wave problems. *Proc. 15th Coastal Engineering Conference,* Honolulu, pp. 2717-2736.

27. Isaacson, M. de St. Q. 1981. Nonlinear wave forces on large offshore structures. Coastal/Ocean Engineering report, Dept. of Civil Engineering, University of British Columbia.

28. Kellogg, O.D. 1929. *Foundations of Potential Theory.* Springer, Berlin.

29. Kim, W.D. 1965. On the harmonic oscillation of a rigid body on the free surface. *J. Fluid Mech.* **21**, pp. 427-451.

30. Korvin-Kroukovsky, B.V. 1955. Investigation of ship motions in regular waves. *Trans. SNAME.* **63**, pp. 386-435.

31. Lambrakos, K.F. 1982. Marine pipeline dynamic response to waves from directional wave spectra. *Ocean Engineering.* **9**(4), pp. 385-405.

32. Leblanc, L.R. and Middleton, F.H. 1982. Pitch-roll buoy wave directional spectra analysis. In *Measuring Ocean Waves,* Natl. Acad. Press, Washington, D.C., pp. 181-193.

33. Leonard, J.W., Huang, M.-C., and Hudspeth, R.T. 1983. Hydrodynamic interference between floating cylinders in oblique seas. *Applied Ocean Research.* 5(3), pp. 158-167.

34. Longuet-Higgins, M.S., Cartwright, D.E., and Smith, N.D. 1961. Observations of the directional spectrum of sea waves using the motions of a floating buoy. In *Ocean Wave Spectra,* Prentice-Hall, Englewood Cliffs, New Jersey, pp. 111-132.

35. MacCamy, R.C. 1964. The motions of cylinders of shallow draft. *J. Ship Research.* 7(3), pp. 1-11.

36. Mitsuyasu, H. *et al.* 1975. Observations of the directional spectrum of ocean waves using a cloverleaf buoy. *J. Phys. Oceanography.* 5, pp. 750-760.

37. Mogridge, G.R. and Jamieson, W.W. 1976. Wave forces on square caissons. *Proc. 15th Coastal Engineering Conference,* Honolulu, pp. 2271-2289.

38. Morison, J.R., O'Brien, M.P., Johnson, J.W., and Schaaf, S.A. 1950. The forces exerted by surface waves on piles. *Petroleum Trans., AIME,* **189**, pp. 149-157.

39. Newman, J.N. 1962. The exciting forces on fixed bodies in waves. *J. Ship Research.* **6**(3), pp. 10-17.

40. Newman, J.N. 1977. *Marine Hydrodynamics.* MIT Press, Cambridge, Massachusetts.

41. Panicker, N.N. 1971. Determination of directional spectra of ocean waves from ocean arrays. Rep. HEL1-18, Hydrogr. Eng. Lab., Univ. of California, Berkeley.

42. St. Denis, M. and Pierson, W.J. 1953. On the motions of ships in confused seas. *Trans. SNAME.* **61**, pp. 280-357.

43. Sand, S.E. 1980. Three-dimensional deterministic structure of ocean waves. Series paper 24, Inst. Hydrody. and Hydraulic Eng., Tech. Univ. of Denmark.

44. Sarpkaya, T. and Isaacson, M. 1981. *Mechanics of Wave Forces on Offshore Structures.* Van Nostrand Reinhold, New York.

45. Shinozuka, M., Fang, S.-L.S., and Nishitani, A. 1979. Time-domain structural response simulation in a short-crested sea. *J. Energy Res. Tech., Trans. ASME,* **101**, pp. 270-275.

46. Ursell, F. 1949. On the heaving motion of a circular cylinder on the surface of a fluid. *Quart. J. Mech. Appl. Math.* **2**, pp. 218-231.

APPENDIX I

ANALYSIS TO DETERMINE OPTIMUM RADIATION DISTANCE

Consider the oblique waves generated by the oscillation of an infinitely long cylinder in any one of its three modes with each mode of motion periodic in time as well as along the axis of the cylinder. The potential associated with the forced motions can be expressed as

$$\Phi(x,y,z,t) = \mathrm{Re}[\phi(x,z)\ \exp\{i(ky\sin\beta-\omega t)\}] \qquad (I1)$$

where k is the wavenumber which is related to the angular frequency ω by the dispersion relation (eqn. 2.11). The two-dimensional potential $\phi(x,z)$ can be expressed in terms of an eigenfunction expansion as

$$\phi(x,z) = A_0 \frac{\cosh[k(z+d)]}{\cosh(kd)} \exp(ikx\cos\beta) + \sum_{m=1}^{\infty} A_m \frac{\cos[k_m(z+d)]}{\cos(k_m d)} \exp(-k_m^* x) \qquad x\geq 0 \qquad (I2)$$

where k_m and k_m^* are wavenumbers defined by

$$-k_m \tan(k_m d) = \frac{\omega^2}{g} \qquad (I3)$$

and

$$k_m^* = [k_m^2 + (k\sin\beta)^2]^{1/2} \qquad (I4)$$

A_0 is the complex amplitude of the potential at the far field and the coefficients A_m are included to account for the evanescent modes of wave motion near the cylinder.

Since the lowest eigenvalue k_1^* gives the slowest decay amongst all the evanescent modes, a decay factor can be defined as

$$d(x) = \exp(-k_1^* x) \tag{I5}$$

where

$$\frac{\pi}{2} < k_1^* d < \pi \tag{I6}$$

In order to achieve a decay rate of $\exp(-2\pi)$ or 0.01 times the value at x=0, the infinite boundary is truncated at a distance X_R given by

$$X_R = \frac{2\pi}{[(k\sin\beta)^2 + (k_1^*)^2]^{1/2}} \tag{I7}$$

A maximum distance of four times the depth is obtained when $k_1^* d = \pi/2$ and $\beta=0°$. The above approximation was found to give good results in water of finite depth. In deep water, eqn. (I7) gives a distance which is too large. Bai (1975) noted that an eigenfunction expansion cannot be used in water of infinite depth for $\beta=0°$. A pulsating source should rather be used to obtain useful information about the optimum distance for truncation of the infinite boundary. The following empirical expression for the radiation distance is used in this study for deep water conditions

$$X_R = \frac{\pi}{[(k\sin\beta)^2 + (\pi/ma)^2]^{1/2}} \tag{I8}$$

where a is the half-beam of the cylinder and m is given as

$$m = \begin{cases} 7 & ka<0.5 \\ 5 & 0.5 \leq ka<1.5 \\ 3 & ka \geq 1.5 \end{cases} \qquad (I9)$$

ka	β°	$\mu_{11}/\rho a^2$		$\lambda_{11}/\rho\omega a^2$	
		present results	GAR	present results	GAR
0.25	5	1.97	2.10	0.57	0.60
	35	2.04	2.16	0.46	0.53
	55	2.08	2.21	0.30	0.38
0.75	5	1.00	0.93	1.31	1.39
	35	1.14	1.19	1.40	1.51
	55	1.84	1.74	1.44	1.56
1.25	5	0.45	0.43	0.93	0.99
	35	0.61	0.59	1.01	1.14
	55	1.09	0.93	1.34	1.40

Table 1. Comparison of the sway added mass and damping coefficients of a semi-circular cylinder ($d/a=\infty$) obtained in the present study with the results of GAR (Garrison,1984)

ka	β°	$\mu_{22}/\rho a^2$		$\lambda_{22}/\rho\omega a^2$	
		present results	B&U	present results	B&U
0.25	5	1.38	1.38	1.99	1.96
	35	1.61	1.60	2.51	2.38
	55	2.64	2.32	3.23	3.06
0.75	5	0.97	0.94	0.94	0.88
	35	1.04	1.06	0.93	0.92
	55	1.43	1.32	1.10	1.02
1.25	5	1.01	0.98	0.49	0.44
	35	0.92	0.90	0.39	0.40
	55	0.98	0.90	0.46	0.42

Table 2. Comparison of the heave added mass and damping coefficients of a semi-circular cylinder ($d/a=\infty$) obtained in the present study with the results of B&U (Bolton and Ursell,1973)

		$\lvert C_1 \rvert$		$\lvert \zeta_1 \rvert$	
ka	$\beta°$	present results	GAR	present results	GAR
0.25	5	0.75	0.77	0.18	0.19
	35	0.63	0.65	0.18	0.19
	55	0.44	0.46	0.18	0.19
0.75	5	1.17	1.18	0.85	0.89
	35	1.07	1.11	0.97	1.02
	55	0.94	0.94	1.17	1.26
1.25	5	0.99	0.99	1.19	1.26
	35	0.95	0.95	1.37	1.56
	55	0.91	0.90	1.89	1.96

Table 3. Comparison of the sway exciting force coefficient and wave amplitude ratio of a semi-circular cylinder ($d/a=\infty$) obtained in the present study with the results of GAR (Garrison,1984)

		$\lvert C_2 \rvert$		$\lvert \zeta_2 \rvert$	
ka	$\beta°$	present results	B&U	present results	B&U
0.25	5	1.40	1.40	0.34	0.35
	35	1.41	1.40	0.42	0.43
	55	1.29	1.32	0.58	0.58
0.75	5	0.95	0.94	0.71	0.70
	35	0.87	0.87	0.78	0.80
	55	0.77	0.76	1.02	1.00
1.25	5	0.68	0.67	0.85	0.84
	35	0.54	0.57	0.85	0.87
	55	0.49	0.49	1.10	1.07

Table 4. Comparison of the heave exciting force coefficient and wave amplitude ratio of a semi-circular cylinder (d/a=∞) obtained in the present study with the results of B&U (Bolton and Ursell,1973)

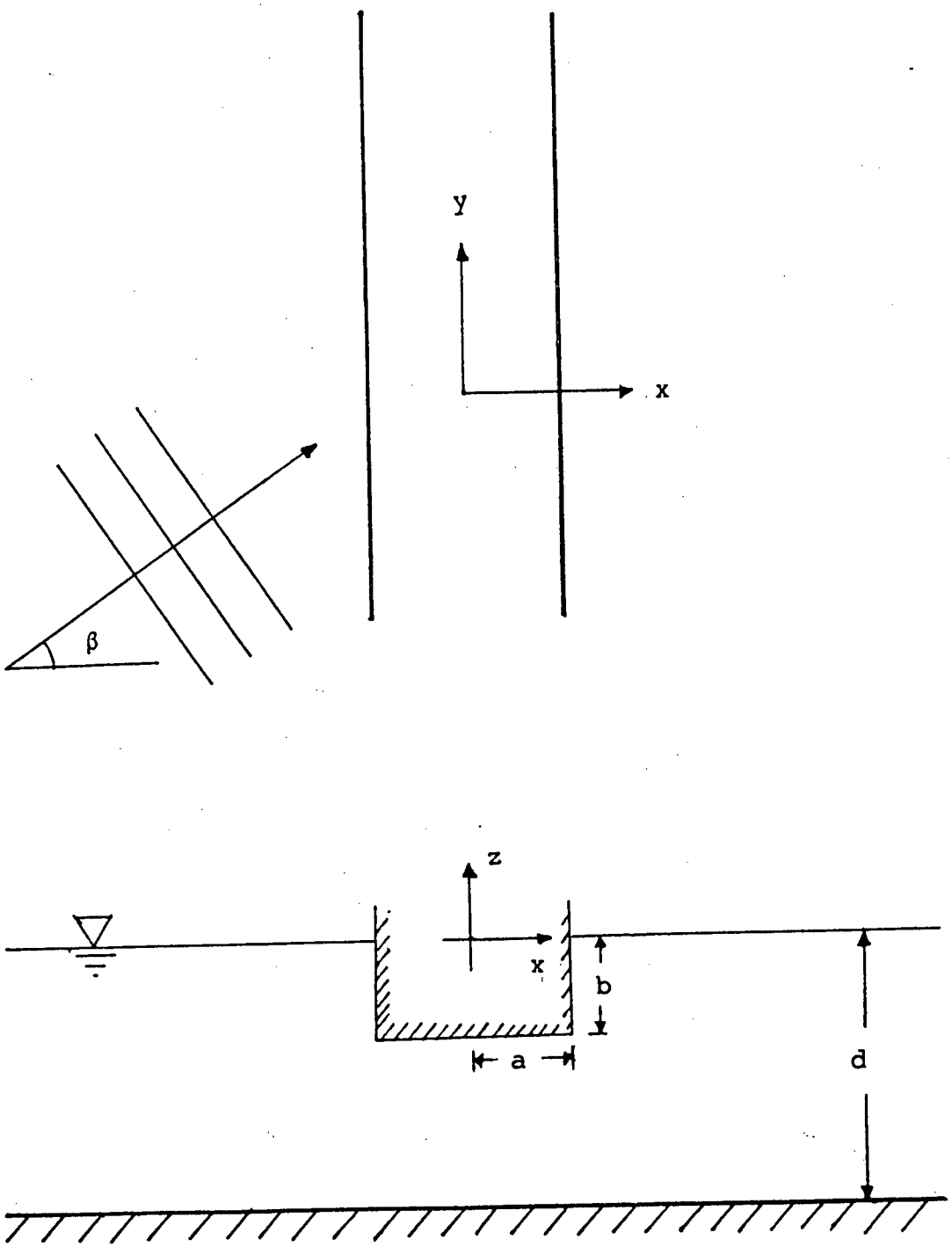

Figure 1. Definition sketch for a rectangular cylinder

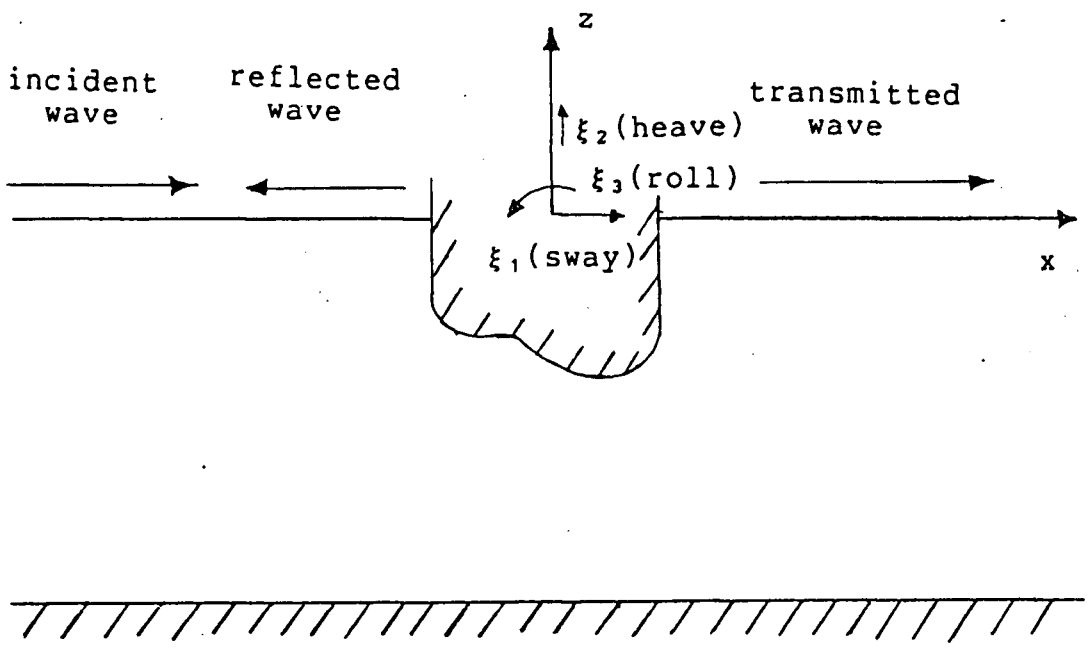

Figure 2. Definition sketch for floating cylinder showing component motions

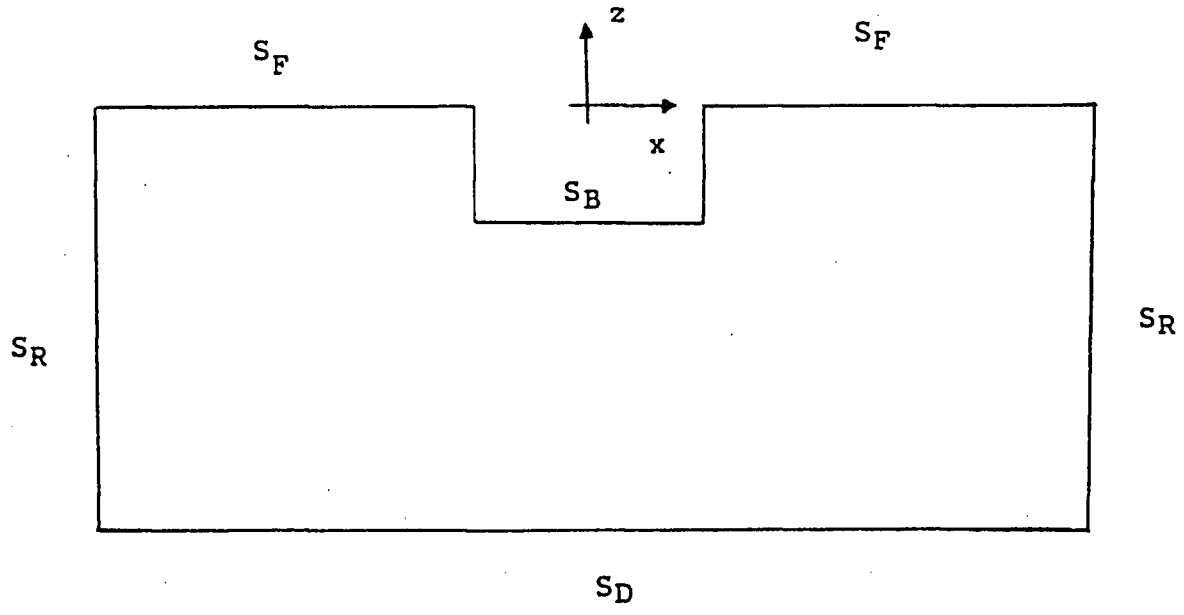

Figure 3. Sketch of closed surface

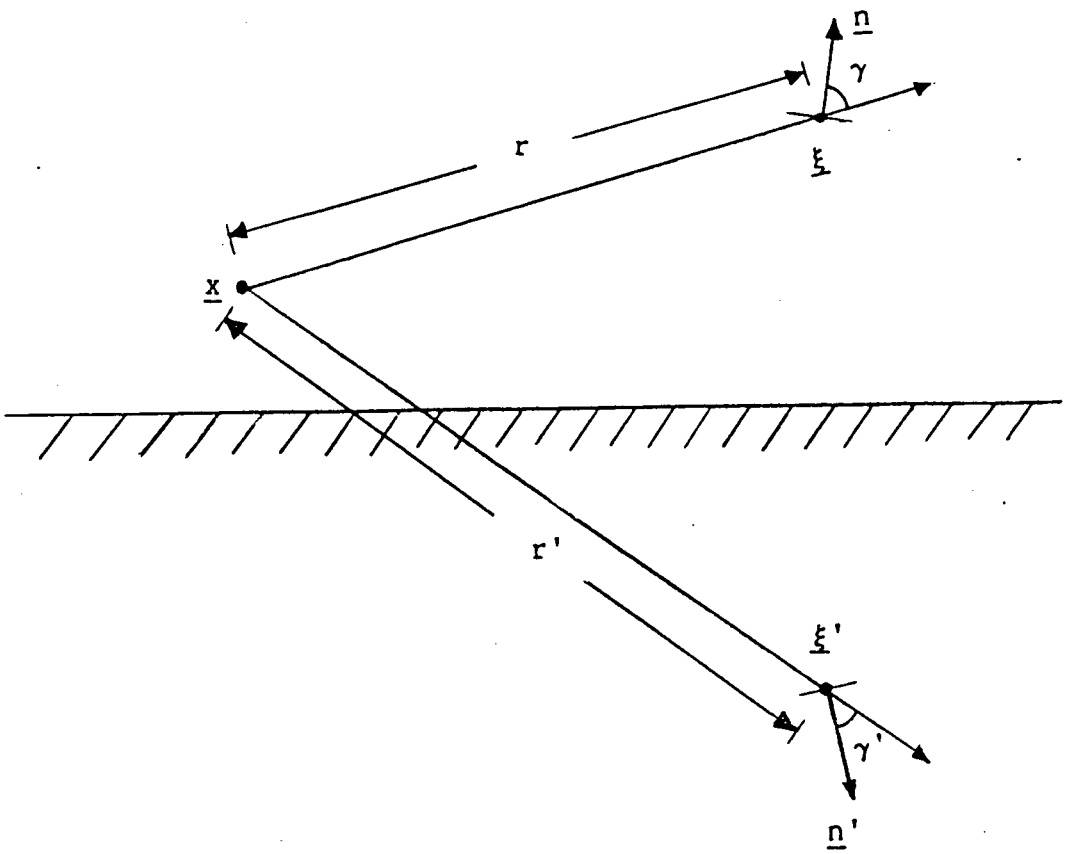

Figure 4. Sketch showing relationship between $\underline{x}$, $\underline{\xi}$, and $\underline{\xi}'$

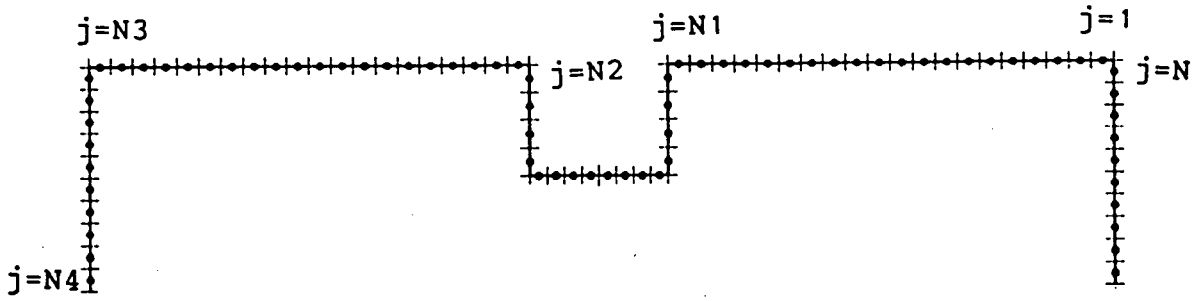

Figure 5. A typical boundary element mesh for a rectangular cylinder (b/a=1,d/a=2)

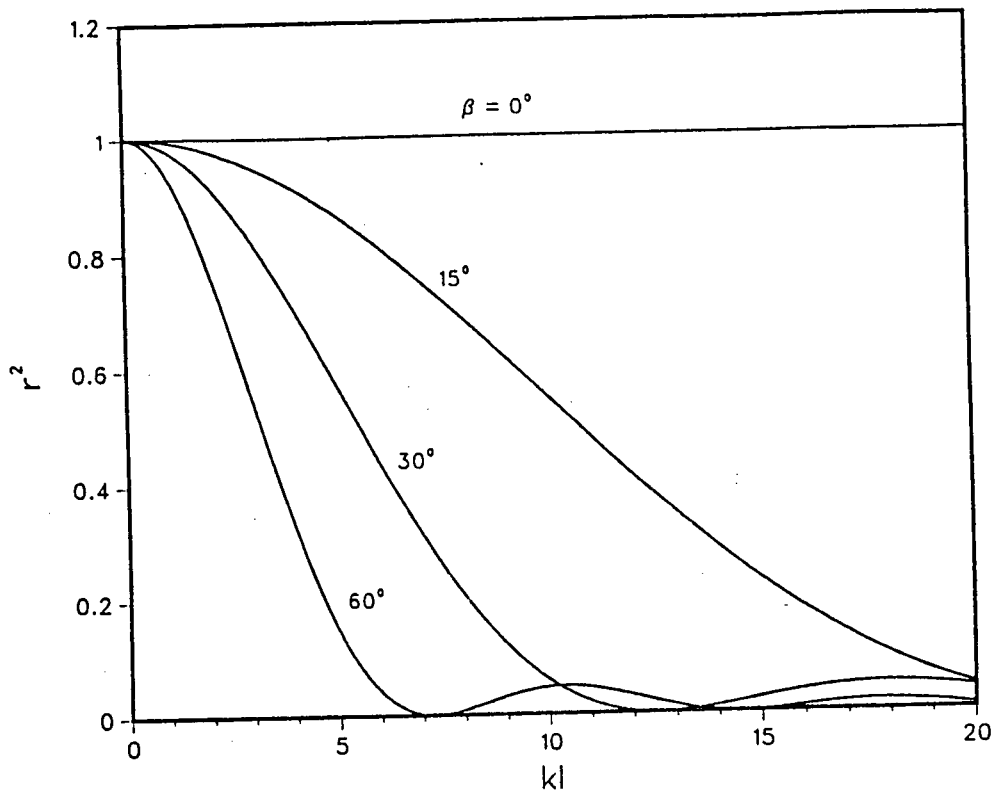

Figure 6. Square of reduction factor r for different values of β

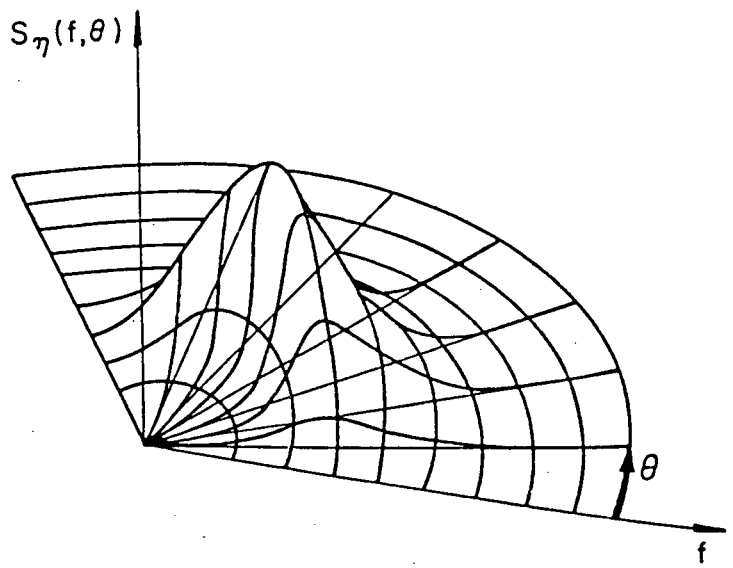

Figure 7. Sketch of a directional wave spectrum

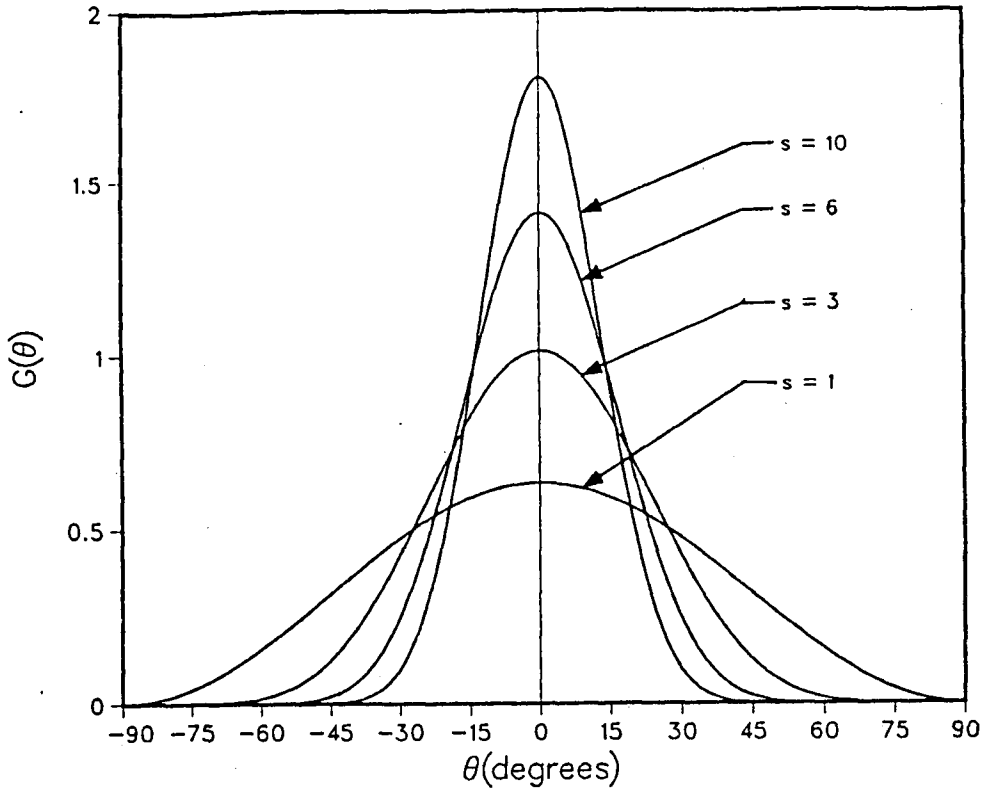

Figure 8. Directional spreading function for different values of the parameter s

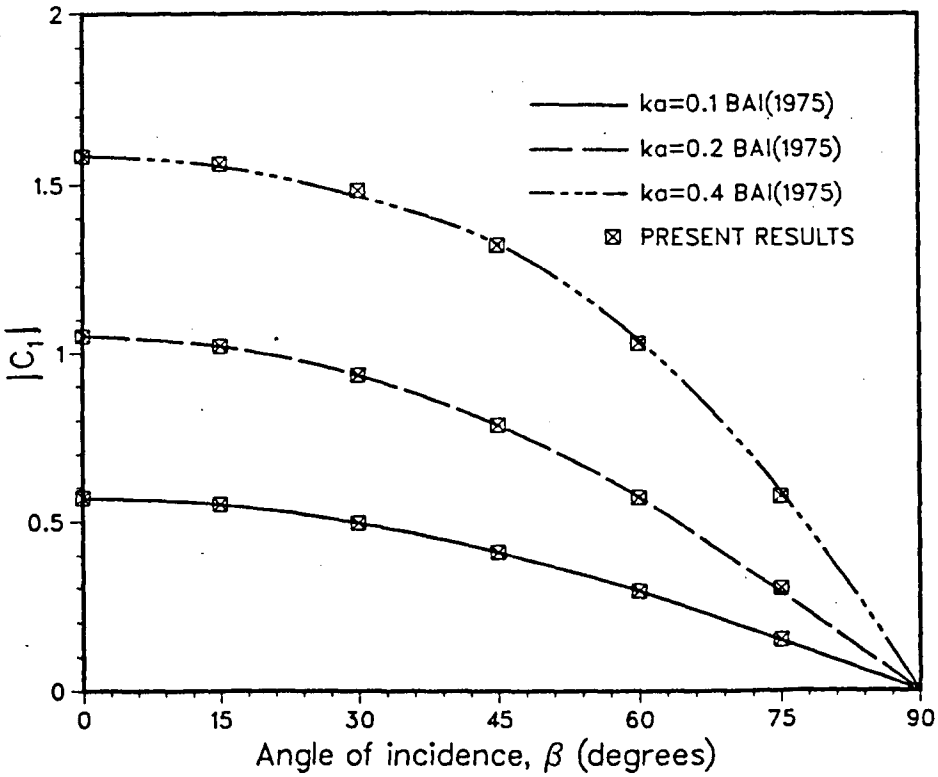

Figure 9. Sway exciting force coefficient for a rectangular cylinder (b/a=1,d/a=2)

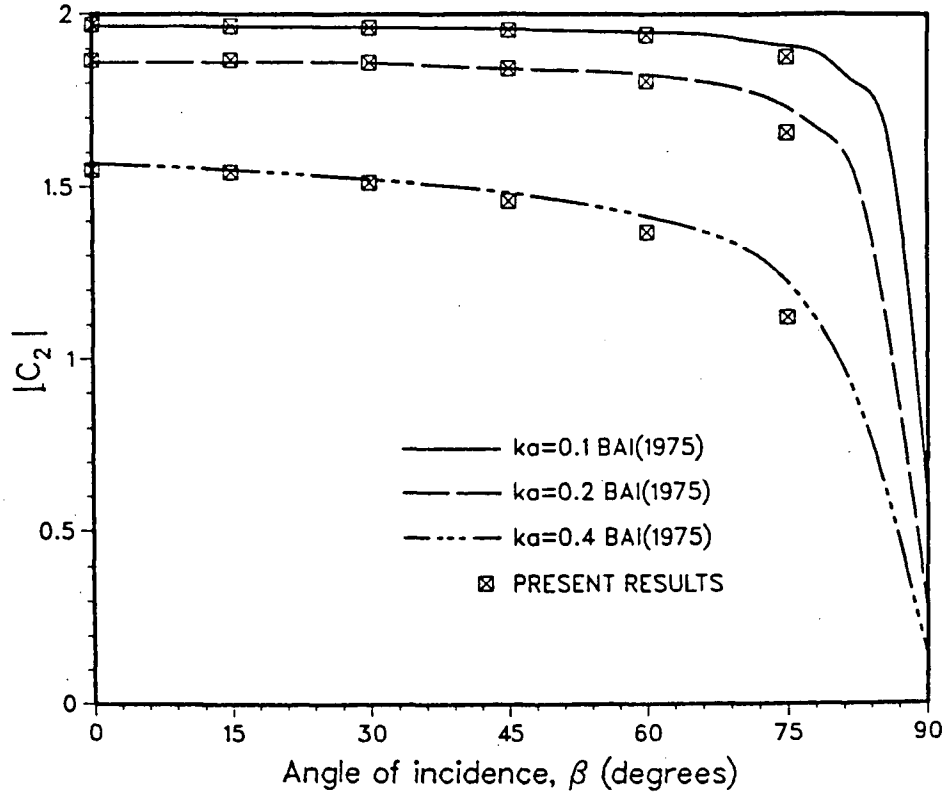

Figure 10. Heave exciting force coefficient for a rectangular cylinder (b/a=1,d/a=2)

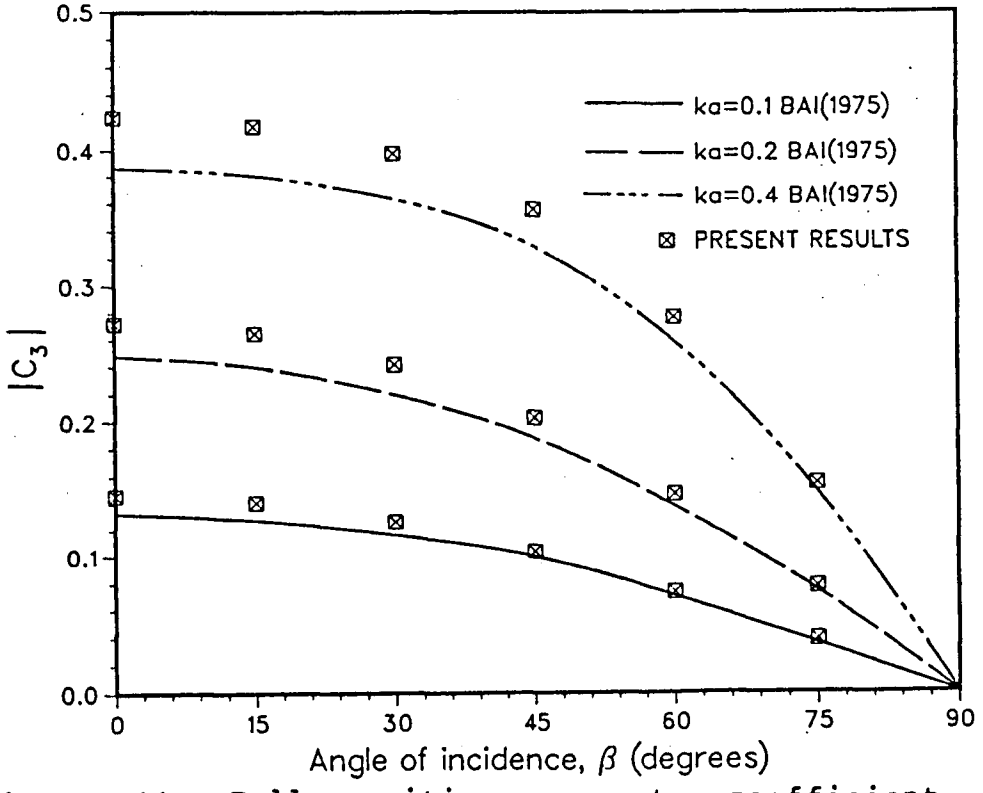

Figure 11. Roll exciting moment coefficient for a rectangular cylinder (b/a=1,d/a=2)

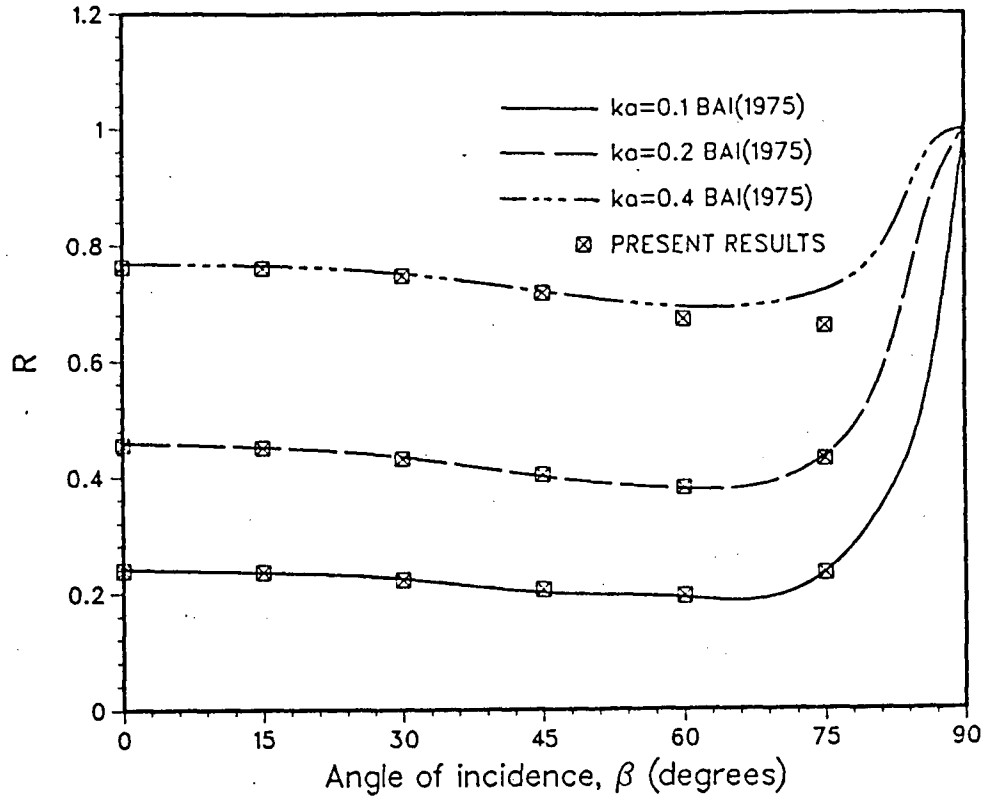

Figure 12. Reflection coefficient for a rectangular cylinder (b/a=1,d/a=2)

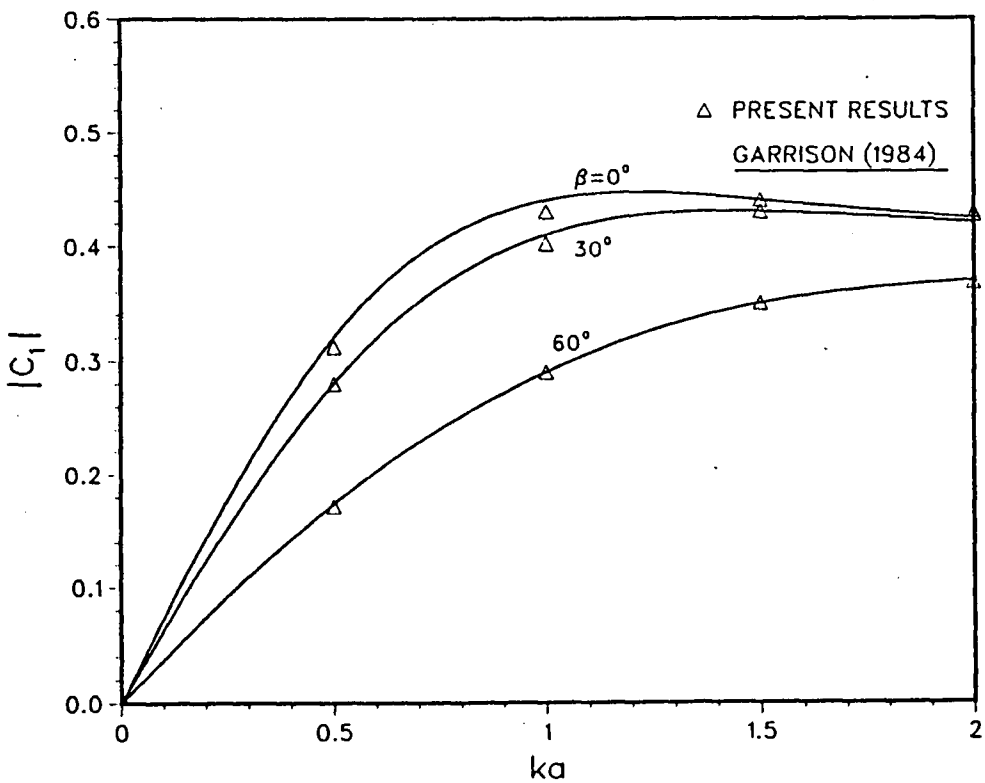

Figure 13. Sway exciting force coefficient for a rectangular cylinder (b/a=0.265,d/a=∞)

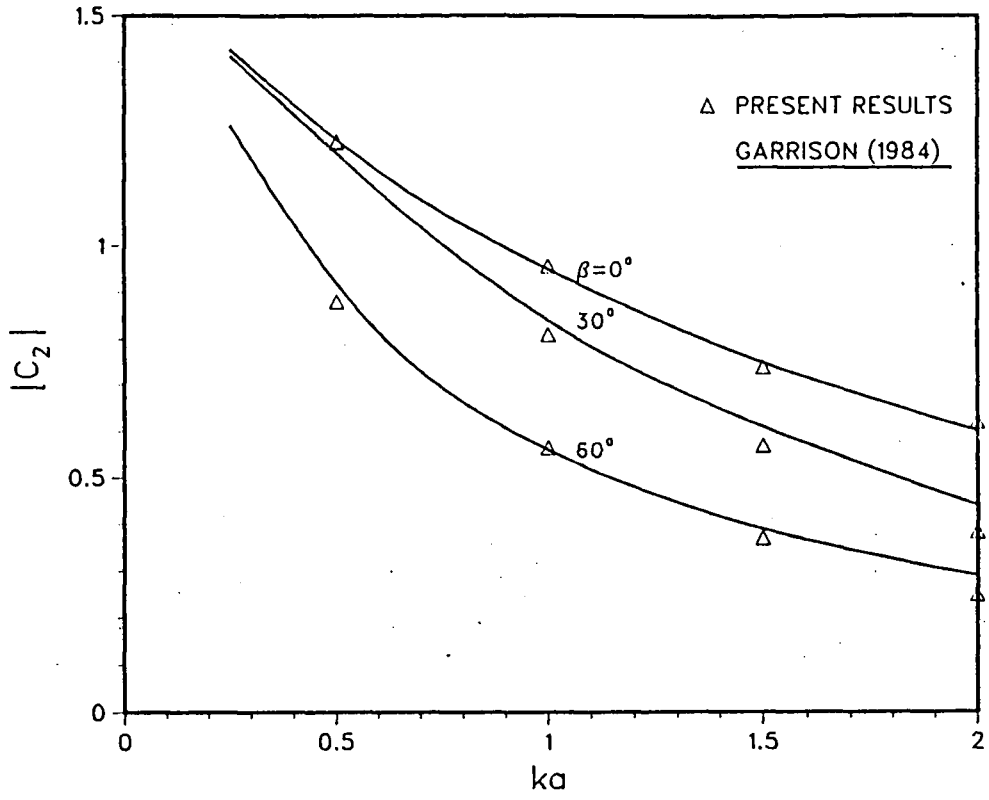

Figure 14. Heave exciting force coefficient for a rectangular cylinder (b/a=0.265,d/a=∞)

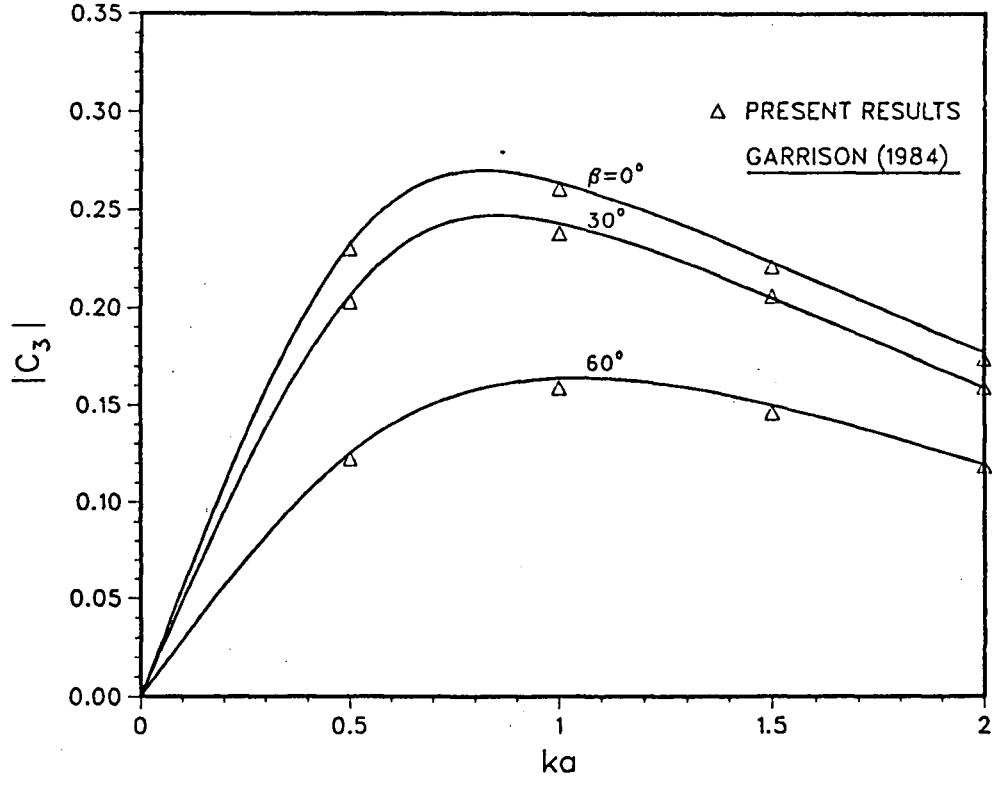

Figure 15. Roll exciting moment coefficient for a rectangular cylinder (b/a=0.265,d/a=∞)

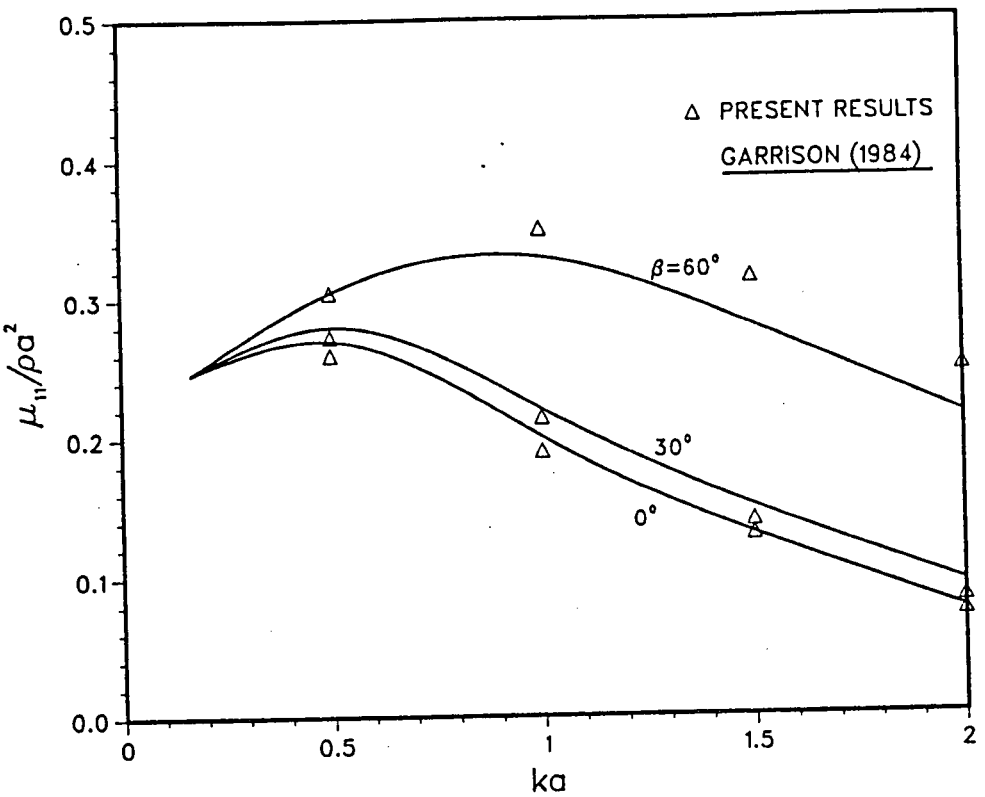

Figure 16. Sway added mass coefficient for a rectangular cylinder (b/a=0.265,d/a=∞)

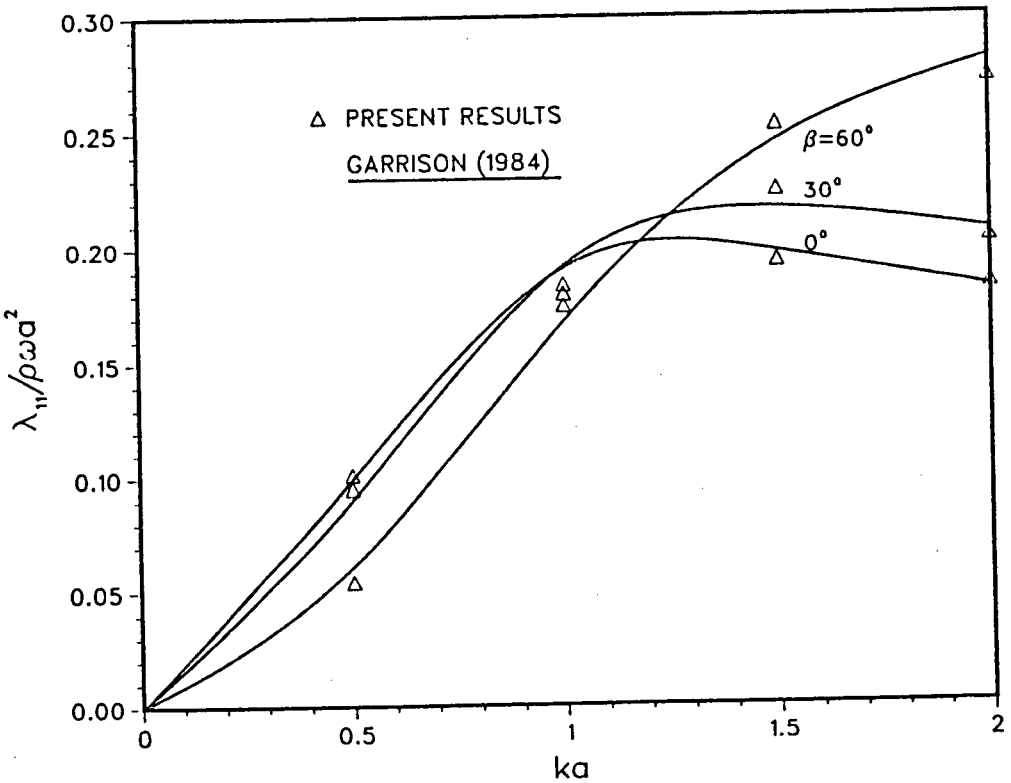

Figure 17. Sway damping coefficient for a rectangular cylinder (b/a=0.265,d/a=∞)

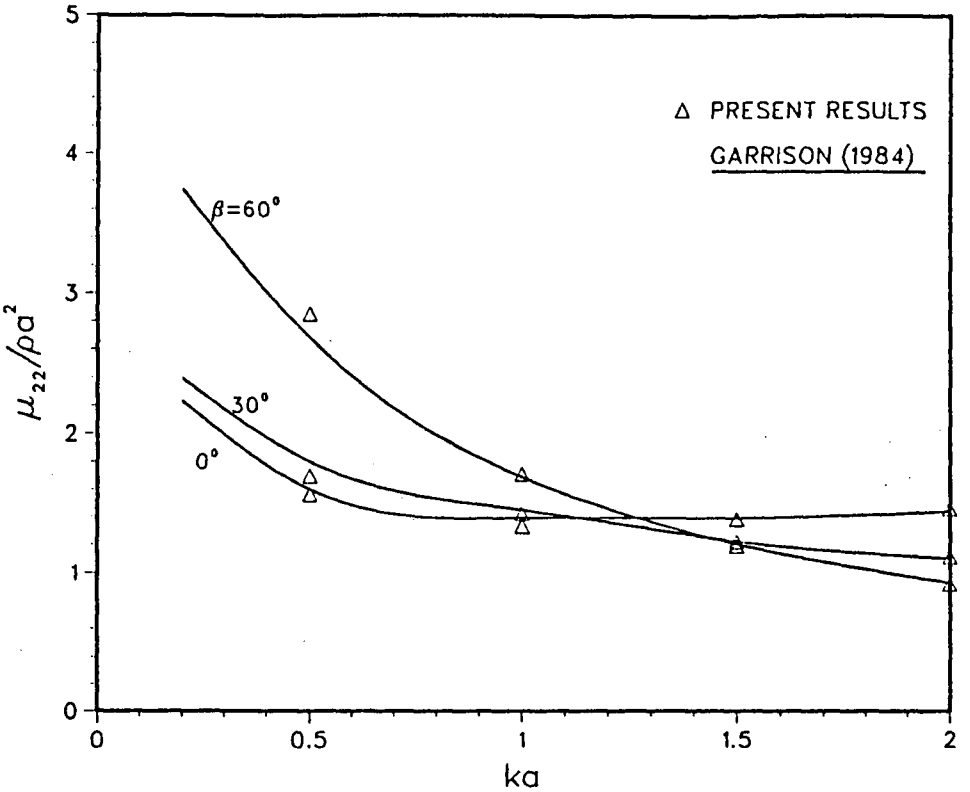

Figure 18. Heave added mass coefficient for a rectangular cylinder (b/a=0.265,d/a=∞)

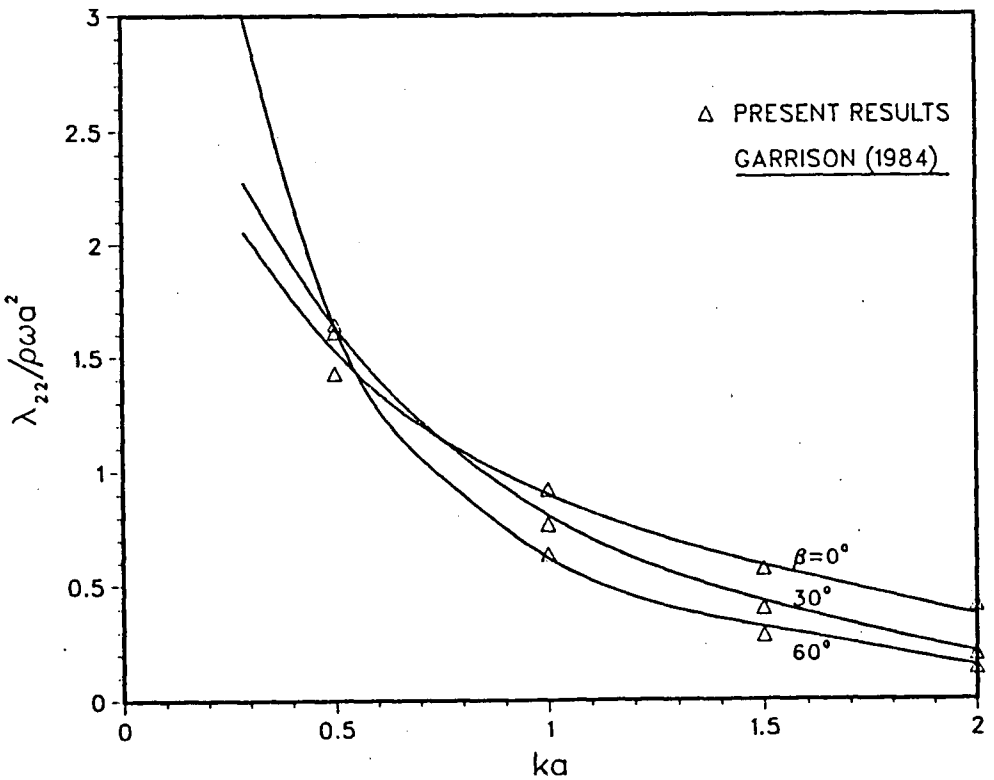

Figure 19. Heave damping coefficient for a rectangular cylinder (b/a=0.265,d/a=∞)

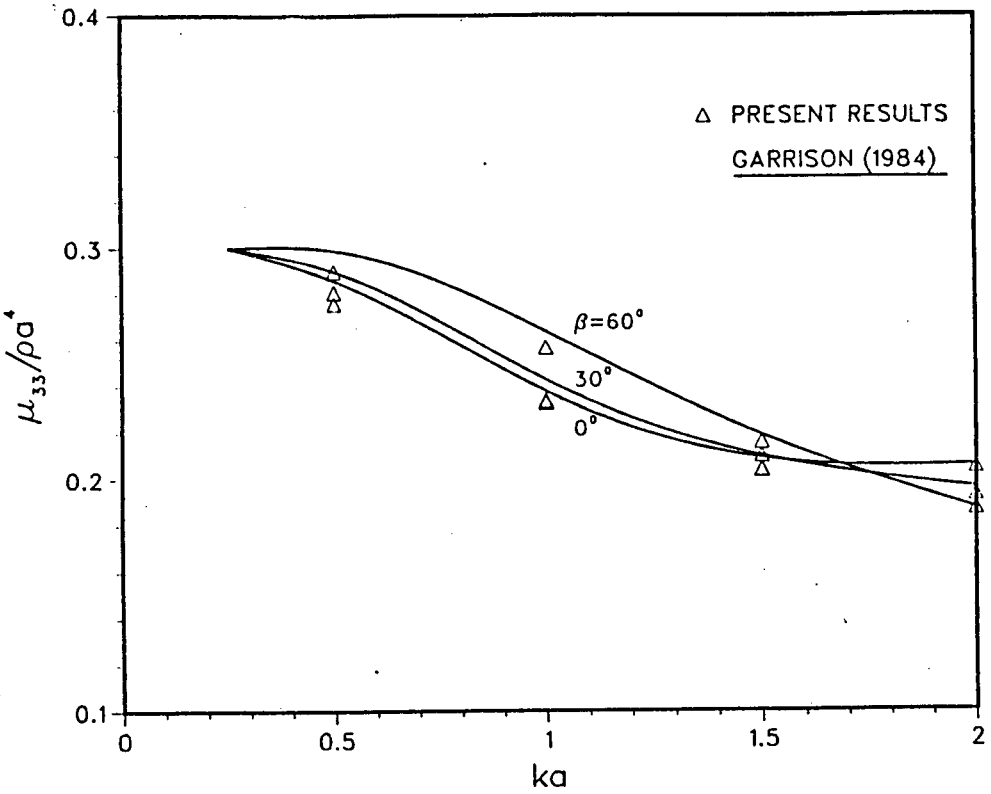

Figure 20. Roll added mass coefficient for a rectangular cylinder (b/a=0.265,d/a=∞)

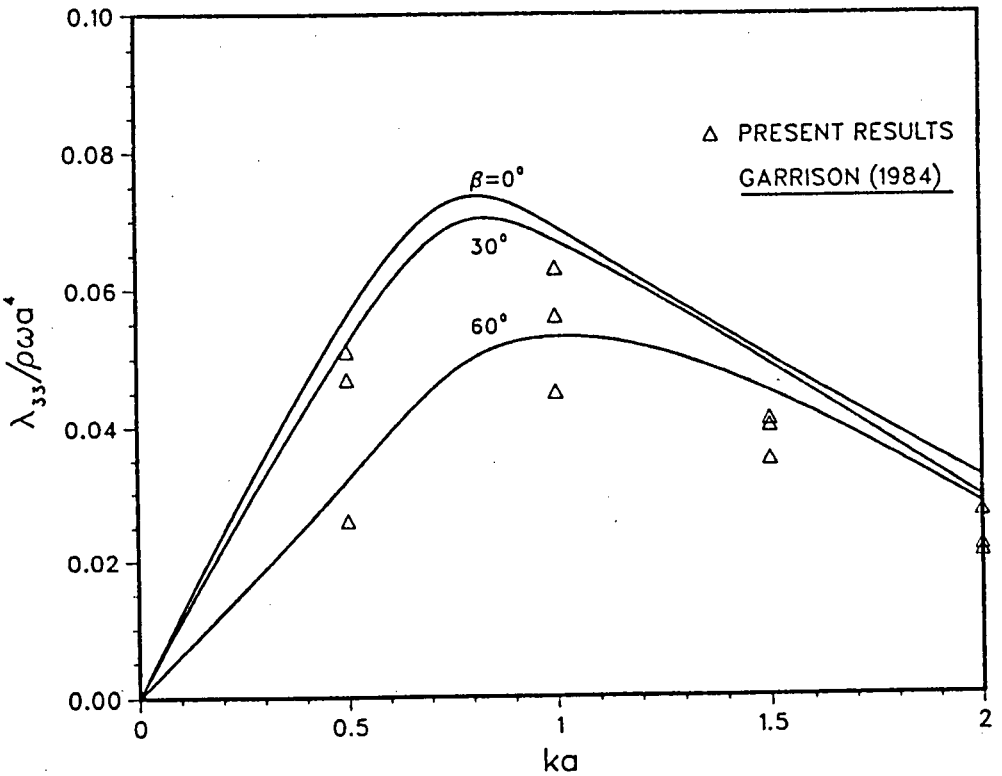

Figure 21. Roll damping coefficient for a rectangular cylinder (b/a=0.265,d/a=∞)

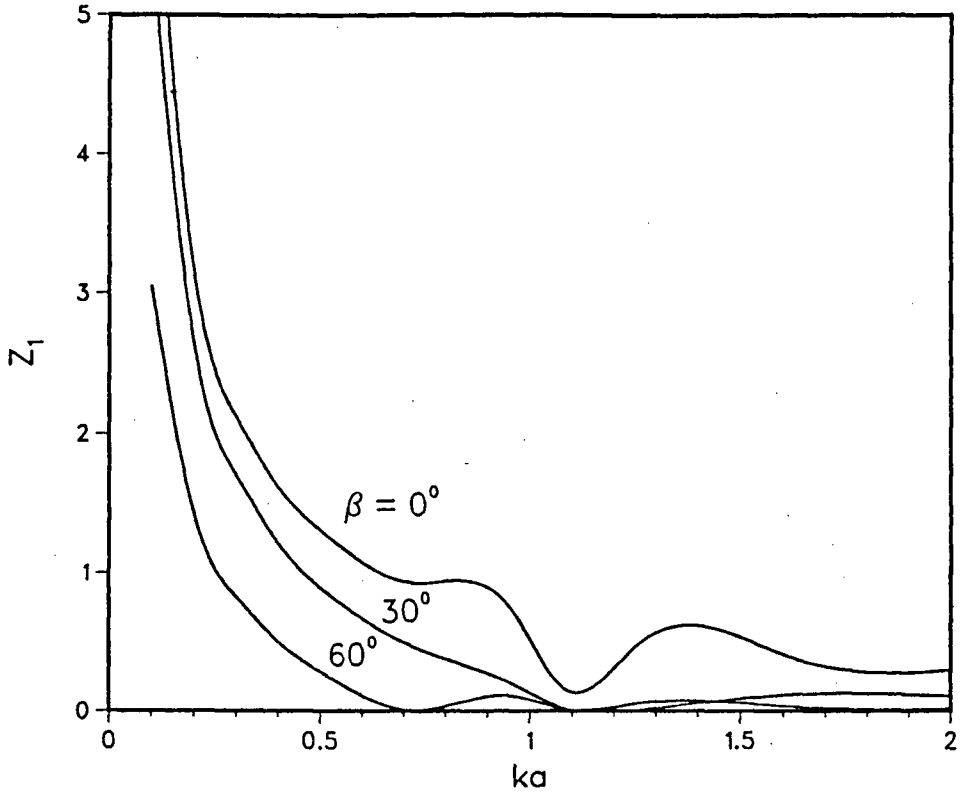

Figure 22. Sway response amplitude operator for a long floating box (a=7.5m,b=3m,l=75m,d=12m)

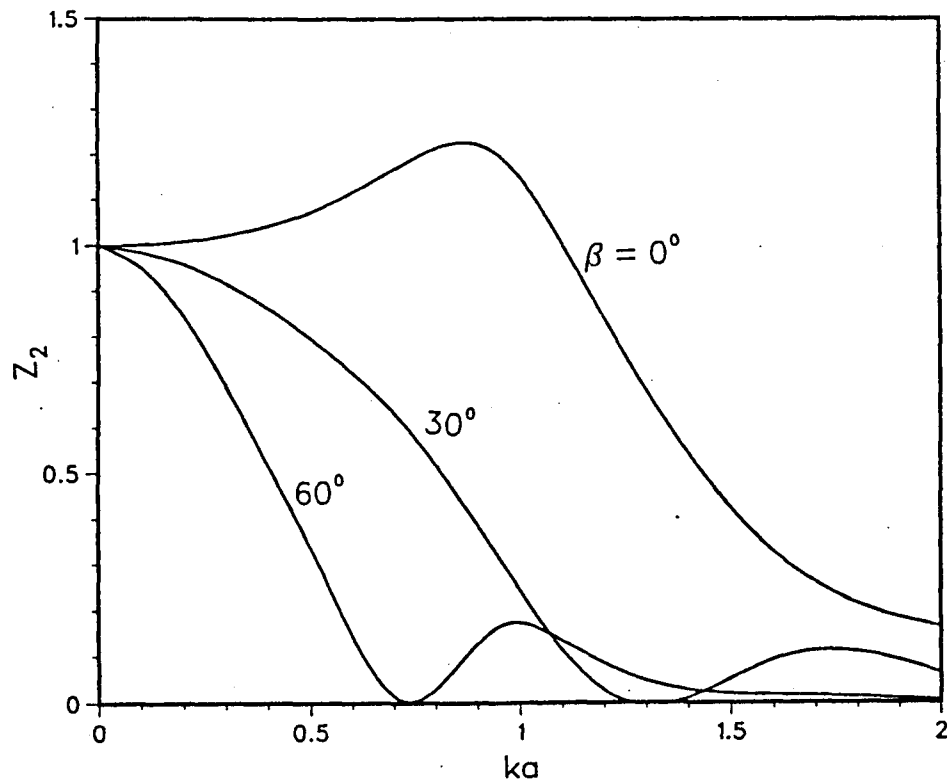

Figure 23. Heave response amplitude operator for a long floating box (a=7.5m,b=3m,l=75m,d=12m)

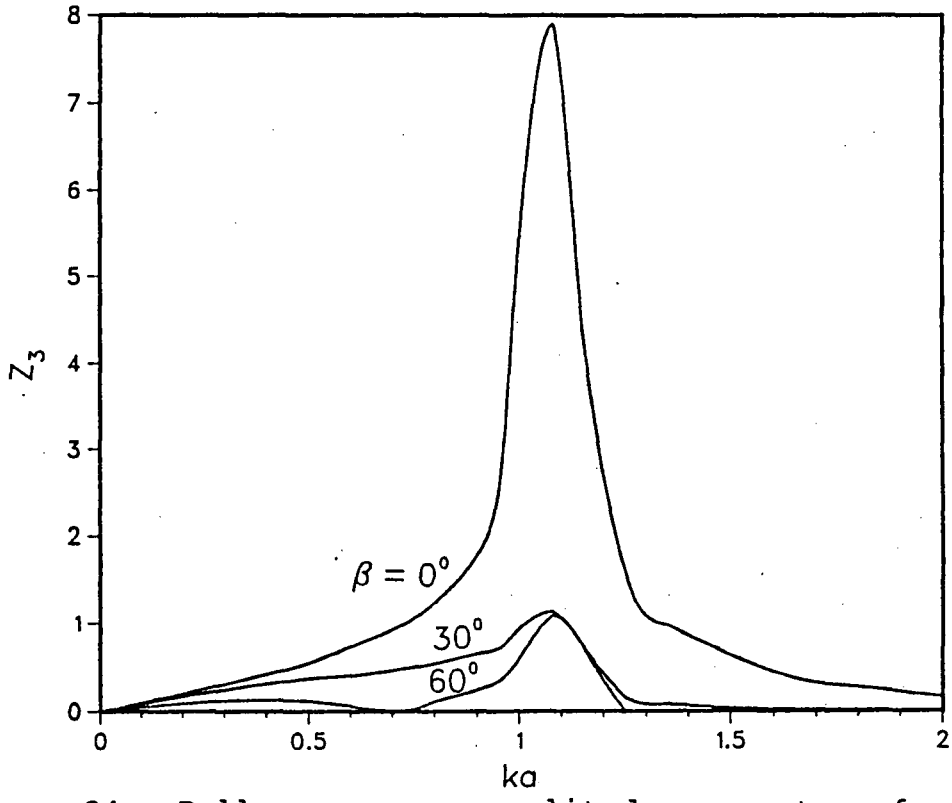

Figure 24. Roll response amplitude operator for a long floating box (a=7.5m,b=3m,l=75m,d=12m)

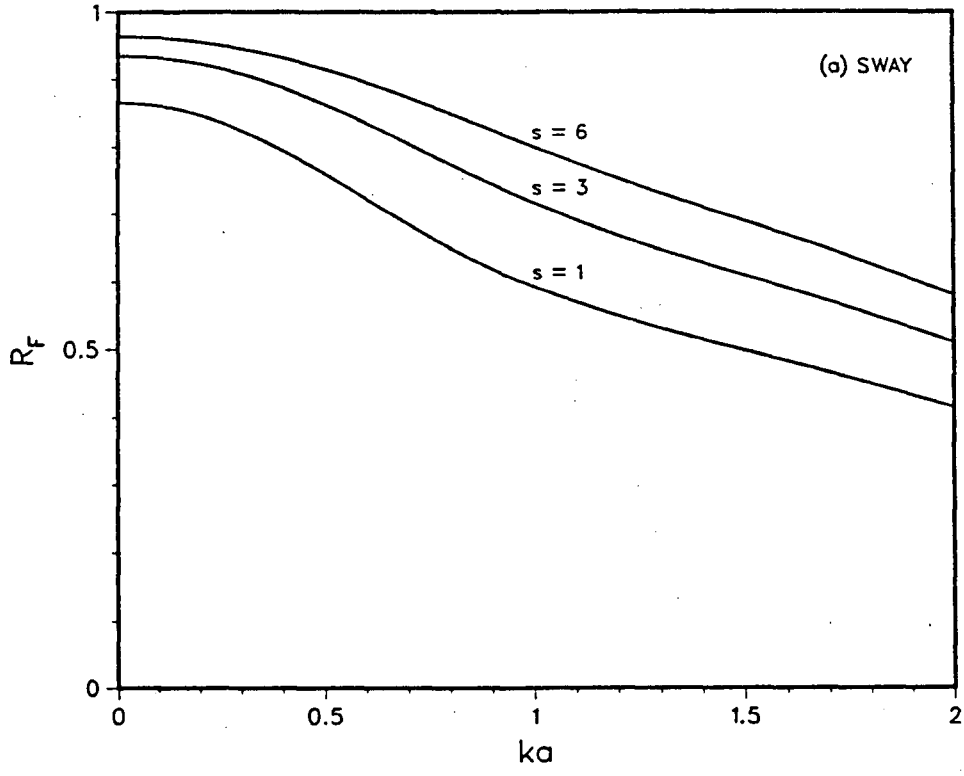

Figure 25. Force and moment reduction factors for a long floating box (a=7.5m,b=3m,l=75m,d=12m)

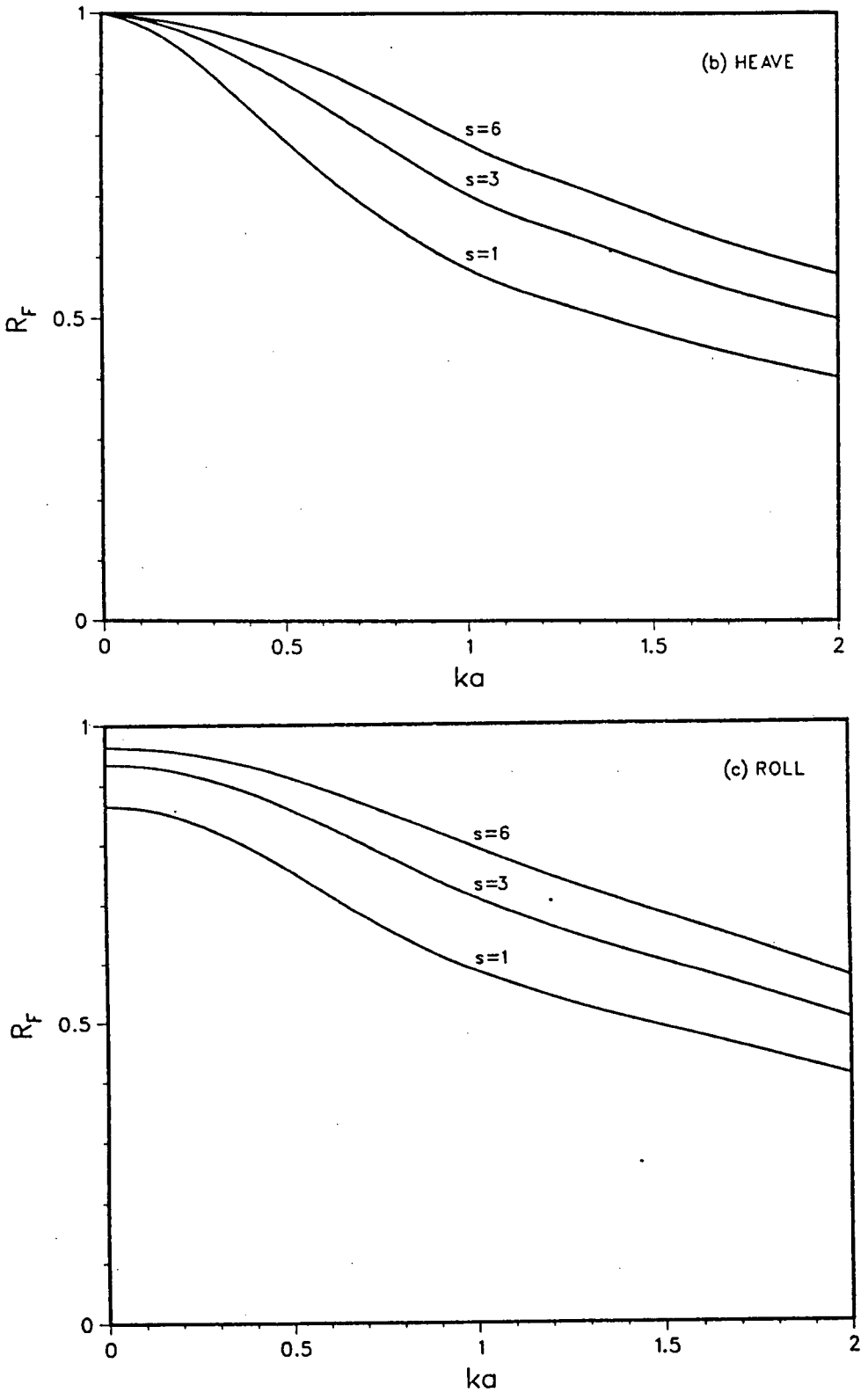

Figure 25.(cont.) Force and moment reduction factors for a long floating box (a=7.5m,b=3m,l=75m,d=12m)

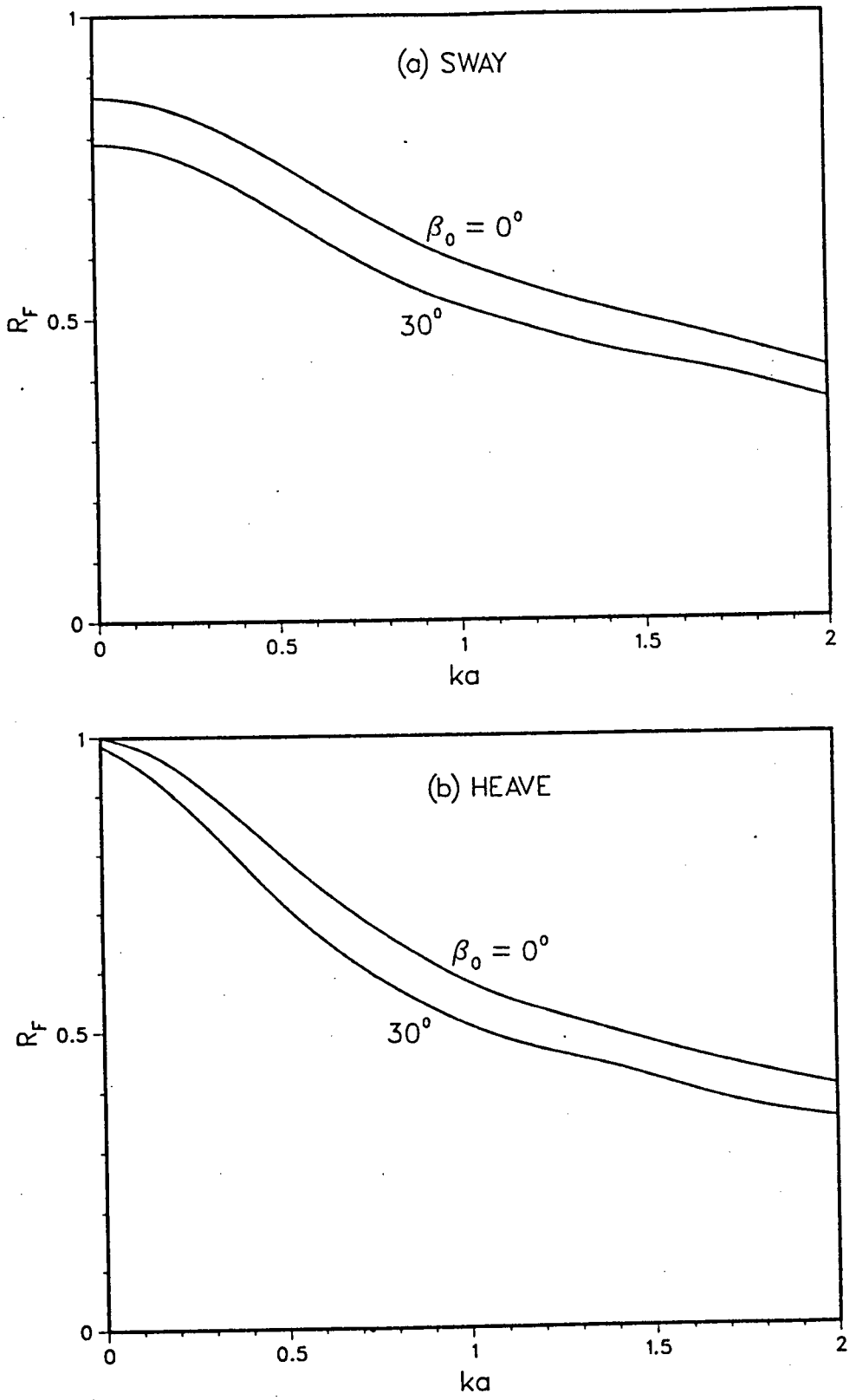

Figure 26. Force reduction factors for a long floating box (a=7.5m,b=3m,l=75m,d=12m) in normal and oblique mean seas

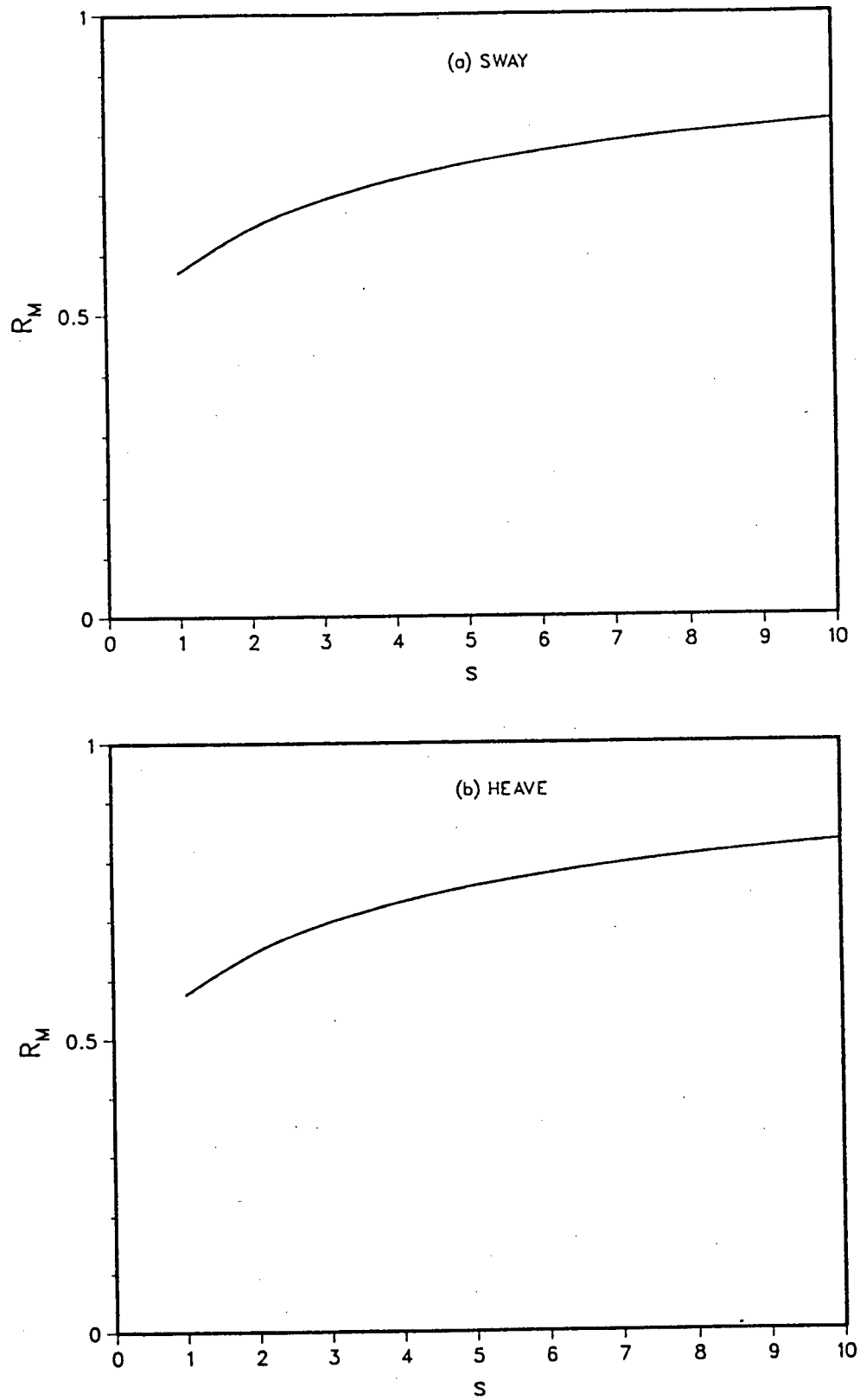

Figure 27. Response ratios for a long floating box (a=7.5m,b=3m,l=75m,d=12m)

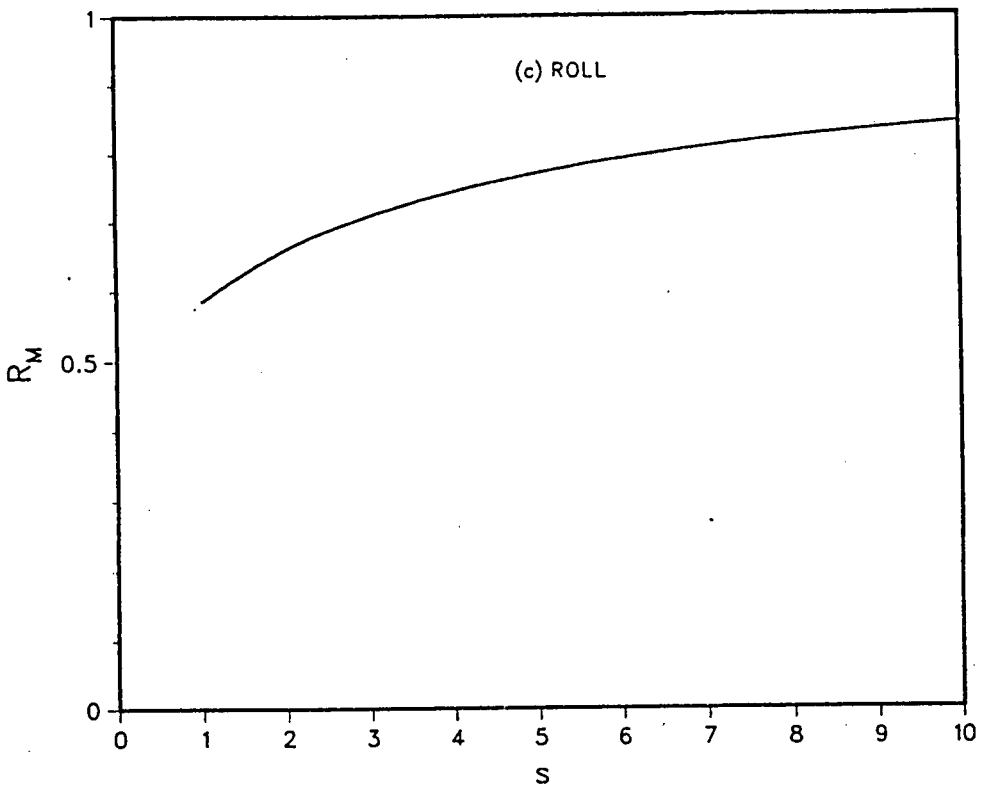

Figure 27.(cont.) Response ratios for a long floating box (a=7.5m,b=3m,l=75m,d=12m)